Conf-950170--2

UCRL- JC-119584
PREPRINT

Can Inertial Electrostatic Confinement Work Beyond the Ion-Ion Collisional Time Scale?

W. M. Nevins

This paper was prepared for
Physics of Spherical Continuous Inertial
Fusion Workshop
Santa Fe, NM
January 12-14, 1995

January 1995

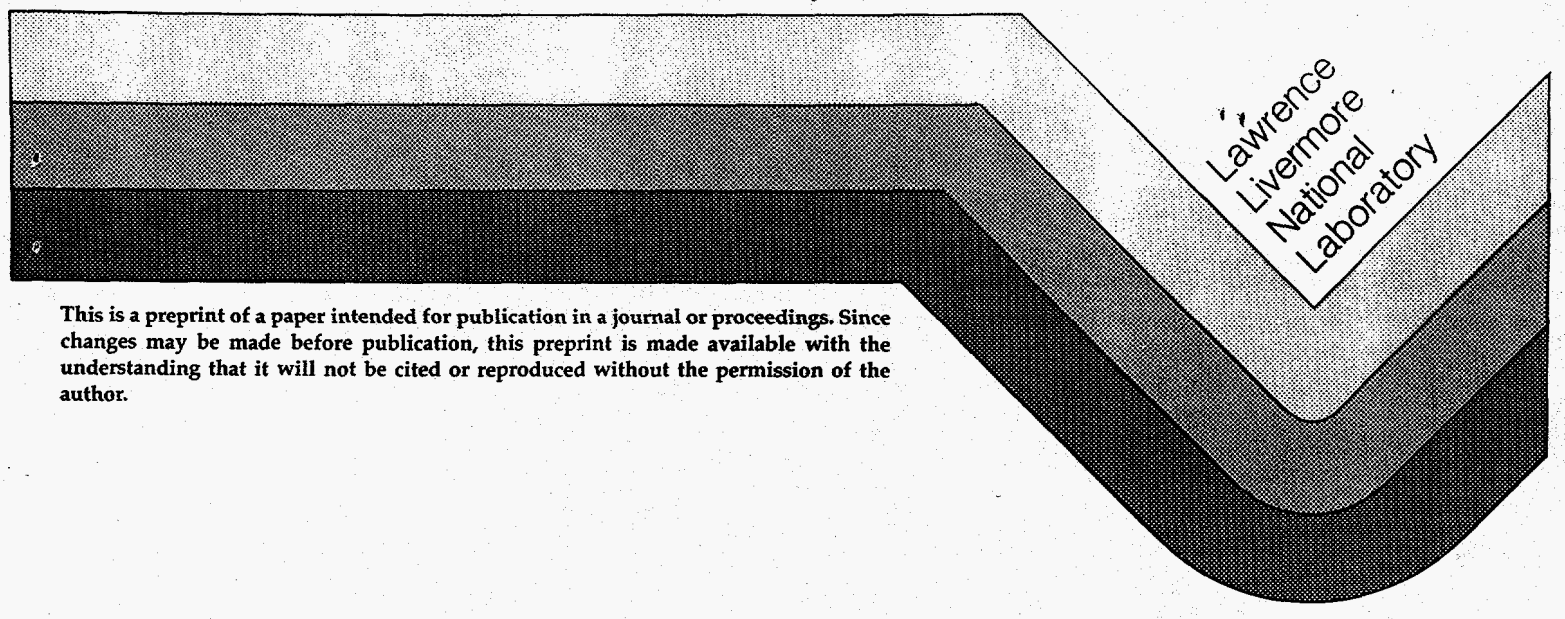

DISCLAIMER

Can Inertial Electrostatic Confinement Work Beyond the Ion-Ion Collisional Time Scale?

W.M. Nevins
Lawrence Livermore National Laboratory
Livermore, CA 94550

January 10, 1995

Abstract

Inertial electrostatic confinement systems are predicated on a non-equilibrium ion distribution function. Coulomb collisions between ions cause this distribution to relax to a Maxwellian on the ion-ion collisional time-scale. The power required to prevent this relaxation and maintain the IEC configuration for times beyond the ion-ion collisional time scale is shown to be at least an order of magnitude greater than the fusion power produced. It is concluded that IEC systems show little promise as a basis for the development of commercial electric power plants.

Can Inertial Electrostatic Confinement Work Beyond the Ion-Ion Collisional Time Scale?

W.M. Nevins
Lawrence Livermore National Laboratory
Livermore, CA 94550

Abstract

Inertial electrostatic confinement systems are predicated on a non-equilibrium ion distribution function. Coulomb collisions between ions cause this distribution to relax to a Maxwellian on the ion-ion collisional time-scale. The power required to prevent this relaxation and maintain the IEC configuration for times beyond the ion-ion collisional time scale is shown to be at least an order of magnitude greater than the fusion power produced. It is concluded that IEC systems show little promise as a basis for the development of commercial electric power plants.

1. Introduction

Inertial electrostatic confinement (IEC) is a concept from the early days of fusion research. Work on magnetic confinement fusion in the Soviet Union was begun by Sakharov and others in response to a suggestion from Lavrent'ev that controlled fusion of deuterium could be achieved in an IEC device.[1] The concept was independently invented in the United States by Farnsworth.[2] Inertial electrostatic confinement schemes require the formation of a spherical potential well. Low energy ions are injected at the edge and allowed to fall into this potential well. If the ion injection energy is low, the ions have a low transverse energy, low angular momentum, and must pass near the center of the spherical potential well on each transit. The repeated focusing of the ions at the center of the well results in peaking of the fuel density and greatly enhances the fusion rate relative to what would be achieved in a uniform plasma of the same volume and stored energy. This strong ion focusing at the center of the potential well is the defining feature of IEC schemes. The plasma configuration envisioned by proponents of IEC fusion systems is illustrated in Fig. 1.

---

[1] A. Sakharov, *Memoirs* (Random House, New York, 1992) p. 139.
[2] R.L. Hirsch, Journal of Applied Physics 38, 4522 (1967).

Figure 1. Plasma Configuration in an IEC Device

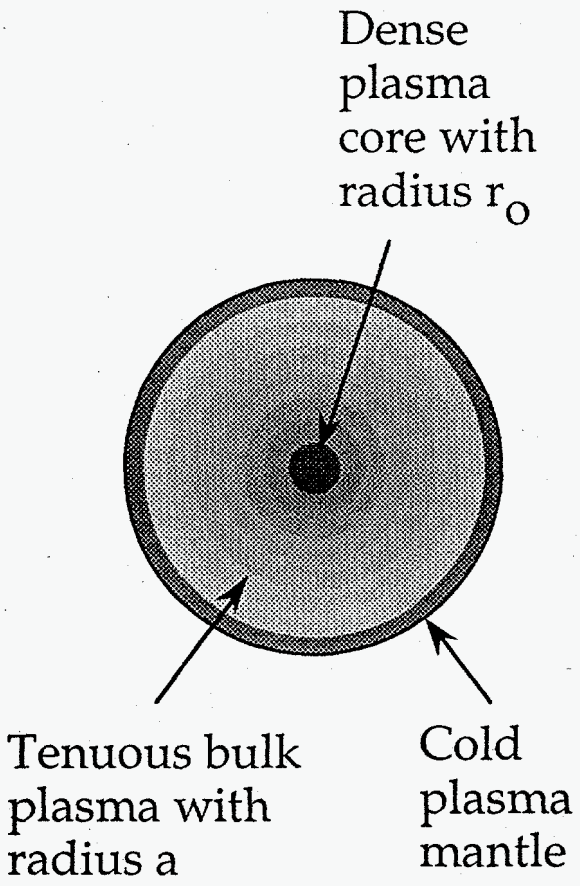

Fig. 1 The IEC plasma is divided into three regions: a dense plasma core, a bulk plasma where the density falls approximately as $1/r^2$, and a cold plasma mantle where the ions are reflected from the edge of the potential well and the mean kinetic energy is low.

Early spherical electrostatic traps[2,3,4] required grids to produce the confining potential. Calculations of grid cooling requirements[5] indicated that this concept would require a grid radius greater than 10 m to achieve net energy output, leading to an impractical reactor. It was suggested that the concept could be improved by using a magnetic field to shield the grid from the hot plasma; and in the Soviet Union the concept evolved into an investigation of electrostatically plugged cusps (see Ref. 6 for an excellent review of this field). In

---

[3] O.A. Lavrent'ev, Ukrain. Fiz. Zh. 8, 440 (1963).

[4] O.A. Lavrent'ev, *Investigations of an Electromagnetic Trap"*, Magnitnye Lovushki Vypusk (Naukova Dumka, Kiev, 1968) 77 [for an English translation, see AEC-TR-7002 (Rev)].

[5] O.A. Lavrent'ev, Ann. N.Y. Acad. Sci. 251, 152 (1975).

[6] T.J. Dolan, Plasma Physics and Controlled Fusion 36, 1539 (1994).

this evolution from a purely electrostatic confinement scheme into an magneto-electrostatic-confinement scheme it appeared that a key advantage had been lost—the confining magnetic field lacked spherical symmetry so the strong ion focus is lost within a few ion transit times because the angular momentum of the ions is not conserved in the absence of spherical symmetry.

Recently, there has been a resurgence of interest in electrostatic confinement fusion.[7] Two new concepts for forming the spherical potential well which do not involve internal grids have been proposed—the Pollywell™ and the Penning trap. In a Penning trap a spherical effective potential well is formed in a rotating frame by a combination of electrostatic and magnetic fields.[8] In the Pollywell™ configuration[9,10,11] a polyhedral magnetic cusp is used to confine energetic electrons. The space-charge of these magnetically confined electrons then creates a potential well to confine the ions.

Table I. Reference IEC Reactor Parameters

Quantity	Symbol	Value
Potential well depth	Φ_o	50.7 keV
Plasma radius	a	1 m
Core radius	r_o	1 cm
Volume averaged density	$\langle n_i \rangle$	0.5×10^{20} m^{-3}
Peak ion density	n_{io}	3.3×10^{23} m^{-3}
Fusion power	P_{fusion}	590 MW

In estimating the importance of collisional effects on an IEC fusion reactor we will use the parameters in Table I. These parameters generally follow those suggested by Bussard[10] and Krall[11]. We have adjusted the operating point somewhat to take account of our more accurate calculation of the fusion reactivity (see Sec. 3) and to ensure that the projected operating point is consistent with the model described in Sec. 2. We assume a DT-fueled IEC reactor because the power balance is most favorable with this fuel and we find power balance to be the critical problem.

---

[7] See, for example, G.L. Kulcinski, Testimony to the House Subcommittee on Energy (April 21, 1994).

[8] D.C. Barnes, R.A. Nebel, and L. Turner, Phys. Fluids B 5, 3651 (1993).

[9] R.W. Bussard, "Medhod and Apparatus for Controlling Charged Particles", U.S. Patent Number 4,826,646 (May 2, 1989).

[10] R.W. Bussard, Fusion Technology **19**, 273 (1991).

[11] N.A. Krall, Fusion Technology **22**, 42 (1992).

In this work a perfectly spherical potential is assumed, thus assuring that the ion focus can be maintained over many ion transit times (about 1 μs for the IEC reactor parameters of Table I). Ion-ion collisions act on a substantially longer time scale. The ion focusing which defines IEC systems is associated with a strong anisotropy in the ion distribution function. Ion-ion collisions tend to reduce this anisotropy on the ion-ion collisional time scale (about 1 s for the IEC reactor parameters of Table I). It is possible to maintain this non-equilibrium ion distribution function with sufficient recirculating power. The object of this paper is to compute the collisional relaxation rates and estimate the recirculating power required to maintain an IEC reactor beyond the ion-ion collisional time scale.

Proponents of IEC systems often assume an ion distribution function that is nearly mono-energetic.[2, 10, 11, 12] There is not a necessary connection between maintaining the ion focus (which results from the dependence of the ion distribution function on angular momentum) and the variation of the ion distribution function with energy. However, some proponents (see especially Ref. 10) believe this to be a second key feature of IEC systems because of the substantial increase in the fusion rate coefficient for a mono-energetic distribution relative to that of a thermal ion distribution (but see section 3 where it is shown that this increase is not significant).

Our approach in analyzing IEC systems is to develop a simple model that contains the essential features described by proponents of IEC systems; and then to use this model as a basis for the calculation of collisional relaxation rates and for estimates of the fusion power produced by the systems and the auxiliary power required to maintain the non-equilibrium IEC configuration. A successful IEC device must maintain a high convergence ratio, a/r_0. We find this to be a useful ordering parameter, and use it freely to identify leading terms in the collisional relaxation rates and power balance.

In section 2 we present a model IEC ion distribution function and show that it reproduces the central features envisioned by proponents of IEC systems. In section 3 we compute the averaged fusion rate coefficient for this distribution and show that it is not substantially greater than that for a Maxwellian distribution with similar mean energy per particle. In section 4 we compute the collisional rate of increase in the angular momentum squared $\langle L^2 \rangle$ (which determines the rate of decay of the ion focus), and the collisional rate of increase in the energy spread of the ion distribution due to collisions in the plasma bulk and core between ions with large relative velocities. In section 5 we compute the collisional rates of change in $\langle L^2 \rangle$ and energy spread due to collisions in the plasma bulk between ions with small relative velocities. Assuming that the ion distribution is initially strongly focused and nearly mono-energetic, this analysis indicates that it will relax on two characteristic collisional time scales. The

[12]M. Rosenberg and N.A. Krall, Physics of Fluids B 4, 1788 (1992).

shortest collisional time is that at which the ion energy distribution evolves towards a Maxwellian while retaining the strong ion focus [$\tau_\varepsilon \sim (r_o/a)\tau_{ii}$, where r_o is the radius of the ion focus, a is the radius of the bulk plasma, and τ_{ii} is the ion-ion collision time evaluated at the volume averaged density]. The ion anisotropy decays on a longer time scale, $\tau_L \sim \tau_{ii}$. Clearly, some intervention is required if the non-thermal ion distribution is to be maintained beyond the ion collisional time scale. In section 6 we analyze two schemes proposed by proponents of IEC systems,[10,12] and conclude that they will not be effective in maintaining the non-thermal ion distribution function. In section 7 we examine two additional schemes for maintaining a non-thermal ion distributions that rely on controlling the life time of ions in the electrostatic trap. We find that these schemes require the recirculating power be at least an order of magnitude greater than the fusion power for the IEC reactor parameters of Table I. In section 8 we conclude that IEC devices show little promise as a means for generating electric power. However, they may be useful as a means of generating 14 MeV neutrons for other applications.

2. The Model

Two constants of the single-particle motion for an ion of species "s" in a spherically symmetric trap are the total energy,

$$\varepsilon \equiv 1/2 m_s v^2 + q_s \phi(r) \tag{1}$$

and the square of the particle's angular momentum,

$$L^2 \equiv (m_s \mathbf{v} \times \mathbf{r})^2. \tag{2}$$

We consider weakly collisional systems, in which the collision frequency (ν) and fusion rate ($n_s \langle \sigma v \rangle_{DT}$) are small compared to the transit frequency (ω_b) in the electrostatic well. At leading order in ν/ω_b, the ion distribution function is then a function of the single-particle constants of motion. We assume an ion distribution function of the form,

$$f_s = f_s(\varepsilon, L^2). \tag{3}$$

The particle density at radius r is then given by

$$n_s(r) = \pi \int d\varepsilon \, dL^2 \frac{\partial(v_r, v_\perp^2)}{\partial(\varepsilon, L^2)} f_s(\varepsilon, L^2) \ , \tag{4}$$

where the Jacobian between velocity space and (ε, L^2)-space is given by

$$\pi \frac{\partial(v_r, v_\perp^2)}{\partial(\varepsilon, L^2)} = \frac{\pi}{m_s^3 r^2 v_r} \tag{5}$$

and

$$v_r(\varepsilon, L^2) = \sqrt{\frac{2}{m_s}(\varepsilon - q_s\phi) - \frac{L^2}{m_s^2 r^2}} \ . \tag{6}$$

Initially, we consider ion distributions that are mono-energetic, and strongly focused at the center of the sphere (i.e., distributions with low angular momentum). A ion distribution function with these properties is

$$f_s(\varepsilon, L^2) = C_s \, \delta(\varepsilon) \, H(L_o^2 - L^2), \tag{7}$$

where C_s is a constant (to be evaluated below), and H(x) is a Heaviside function.

In our calculations we consider a "square-well" potential,

$$\phi(r) = \begin{cases} -\phi_o & r < a \\ +\phi_o & r \geq a \end{cases}$$

A substantial confining potential ($+\phi_o$) is assumed in order to insure that the dominant collisional effect is thermalization of the ion distribution, rather than ion upscatter (in energy) followed by loss from the potential well. The ion number density corresponding to our model distribution function is then

$$n_s(r) = \int_0^{\infty} dL^2 \int_{-q_s\phi_o+L^2/2m_sr^2}^{q_s\phi_o+L^2/2m_sa^2} d\varepsilon \, \frac{\pi}{m_s^3 r^2 v_r} C_s \, \delta(\varepsilon) \, H(L_o^2 - L^2) \qquad (8)$$

$$= \int_0^{\mathrm{Min}(L_o^2, L_r^2)} dL^2 \frac{\pi C_s}{m_s^3 r^2 v_r} \qquad (9)$$

$$= n_{so} \times \begin{cases} 1 & r < r_o \\ \dfrac{r_o^2/r^2}{1 + \sqrt{1 - r_o^2/r^2}} & r > r_o \end{cases} \qquad (10)$$

where

$$n_{so} \equiv \frac{2\pi v_s C_s}{m_s}, \qquad v_s \equiv \sqrt{\frac{2q_s\phi_o}{m_s}}$$

$$L_r \equiv m v_s r, \quad \text{and} \quad r_o \equiv \frac{L_o}{m_s v_s}.$$

We evaluate the constant C_s by noting that the total number of ions in the trap, N_s, is given by

$$N_s = \int_0^\infty 4\pi r^2 \, dr \, n_s(r) \tag{11}$$

$$= \frac{4\pi a^3}{3} n_{so} \left[1 - \left(1 - r_o^2/a^2\right)^{3/2} \right] \tag{12}$$

$$\approx 2\pi r_o^2 a \, n_{so} \qquad (r_o << a) \tag{13}$$

Hence, we find that the central ion density, n_{so}, is given by

$$n_{so} \approx \frac{N_s}{2\pi r_o^2 a} \approx \frac{2}{3}\left(\frac{a}{r_o}\right)^2 \langle n_s \rangle_{Vol} \tag{14}$$

where

$$\langle n_s \rangle_{Vol} \equiv \frac{N_s}{V} \tag{15}$$

is the volume averaged density, and

$$V = \frac{4\pi}{3} a^3 \tag{16}$$

is the volume of the trap. The corresponding value of C_s is

$$C_s \approx \frac{m_s N_s}{4\pi^2 r_o^2 a v_s} . \tag{17}$$

Restricting the ions distribution function to low values of angular momentum, $|L| \leq L_o = m_s v_s r_o$, has the effect of increasing the central ion density relative to what it would be for an isotropic ion velocity distribution by the factor $0.67\ (a/r_o)^2$. This strong dependence of the central ion density on the ion convergence ratio is illustrated in figure 2. We conclude that the model IEC ion distribution function of Eq. (7) reproduces the essential features of inertial electrostatic confinement schemes—electrostatic confinement, strong central peaking of the fuel ion density, and a mono-energetic energy distribution.

Figure 2. $n_s(r)/n_{so}$

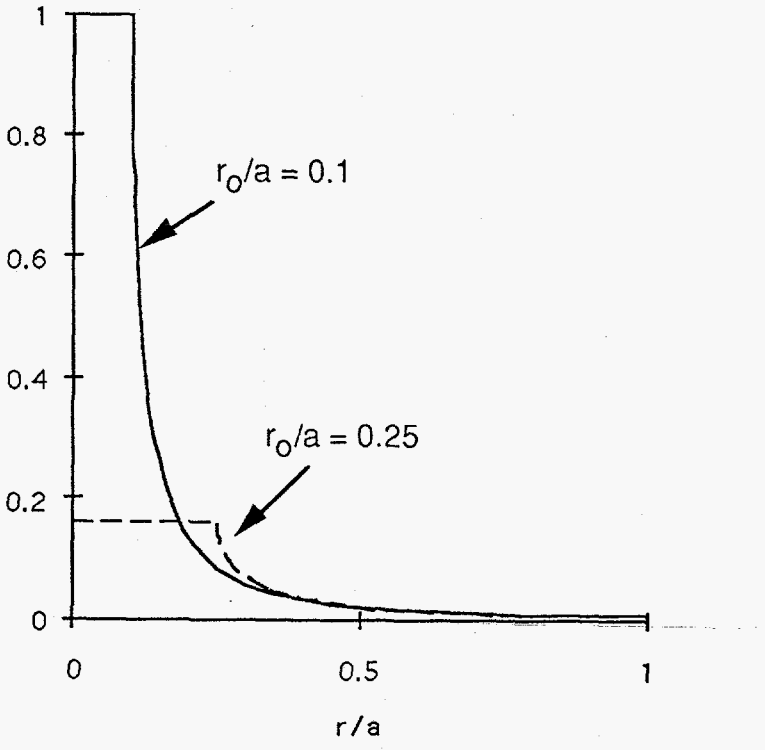

Figure 2 Ion number density plotted versus radius for model IEC ion distribution function in a square-well potential. For the solid curve L_o=0.1 $m_s v_s a$ (corresponding to r_o/a = 0.1) . For the dashed curve L_o=0.25 $m_s v_s a$ (corresponding to r_o/a = 0.25) while N_s, ϕ_o , and a are held fixed. Note the strong dependence of the central ion density on r_o/a.

3. Fusion Power Generation

For a deuterium-tritium plasma, the total fusion power is given by

$$P_{fusion} = Y_{DT} \int d^3r \; n_d(r)\, n_t(r) \langle \sigma v \rangle_{DT}(r) , \tag{18}$$

Where Y_{DT} =17.6 MeV is the fusion yield per event. We assume an equal mixture of deuterium and tritium (with no impurities), and that deuterium and tritium distribution functions have the same convergence ratio, so that

$$n_i(r) = n_d(r) + n_t(r) = 2\, n_d(r) = 2\, n_t(r). \tag{19}$$

If the fusion rate coefficient, $\langle \sigma v \rangle_{DT}$, were independent of radius, then the fusion power would be given by

$$P_{fusion} = \frac{1}{4} Y_{DT} \langle \sigma v \rangle_{DT} \int d^3r \; n_i^2(r) \tag{20}$$

$$\approx \frac{2\pi}{3} \; r_o^3 \, n_{io}^2 \; Y_{DT} \langle \sigma v \rangle_{DT} \left[1 - \frac{3}{8} \frac{r_o}{a} + \ldots \right],$$

where we have used the fact that, for the model distribution described in Sec. 2,

$$\int d^3r \; n_i^2(r) \approx \frac{4\pi}{3} \; r_o^3 \, n_{io}^2 \left[2 - \frac{3}{4} \frac{r_o}{a} + \ldots \right]. \tag{21}$$

This motivates the definition

$$\langle \sigma v \rangle_{DT}^{eff} \equiv \frac{P_{fusion}}{\frac{1}{4} Y_{DT} \int d^3r \; n_i^2(r)} . \tag{22}$$

The radial dependence of the fusion rate coefficient arises because, even for mono-energetic distributions, the fusion rate has to be averaged over the angle between the colliding particles. This angular distribution varies as a function of radius. For the model described in Sec. 2 the angular distribution function $g(\mu)$ is isotropic within the core (i.e., for $r \le r_o$), while outside of the core ($r > r_o$) this distribution satisfies

$$g(\mu) = \begin{cases} \dfrac{1}{2\sqrt{1 - r_o^2/r^2}} & |\mu| > \sqrt{1 - r_o^2/r^2} \\ \\ 0 & |\mu| < \sqrt{1 - r_o^2/r^2} \end{cases} \tag{23}$$

where μ is the cosine of the angle between the ion velocity and the unit vector in the radial direction, $\hat{e}_r$.

The averaged fusion rate coefficient for an ion with zero angular momentum (i.e., an ion for which $\mu = \pm 1$) colliding with a background ions described by the model IEC distribution is

$$\langle \sigma v \rangle_{DT} = \int_{-1}^{1} d\mu \, g(\mu) \, \sigma(E_{cm}) \, v_r(\mu) \tag{24}$$

where the relative velocity v_r satisfies

$$v_r^2(\mu) = v_d^2 - 2\mu v_d v_t + v_t^2 , \tag{25}$$

the center-of-mass energy is given by $E_{cm} = \frac{1}{2} m_r v_r^2$, and the reduced mass by

$$m_r = \frac{m_d m_t}{m_d + m_t} . \tag{26}$$

The μ-integral is evaluated numerically using the analytic fit to the center-of-mass fusion cross-section developed by Bosch and Hale[13] (which is accurate to within 2% over the relevant energy range). The radial variation of the fusion rate coefficient is shown in Fig. 3 for three different well depths, ϕ_o.

[13]H.S. Bosch and G.M. Hale, Nuclear Fusion 32, 611 (1992).

Figure 3. Radial Dependence of $\langle\sigma v\rangle_{DT}$

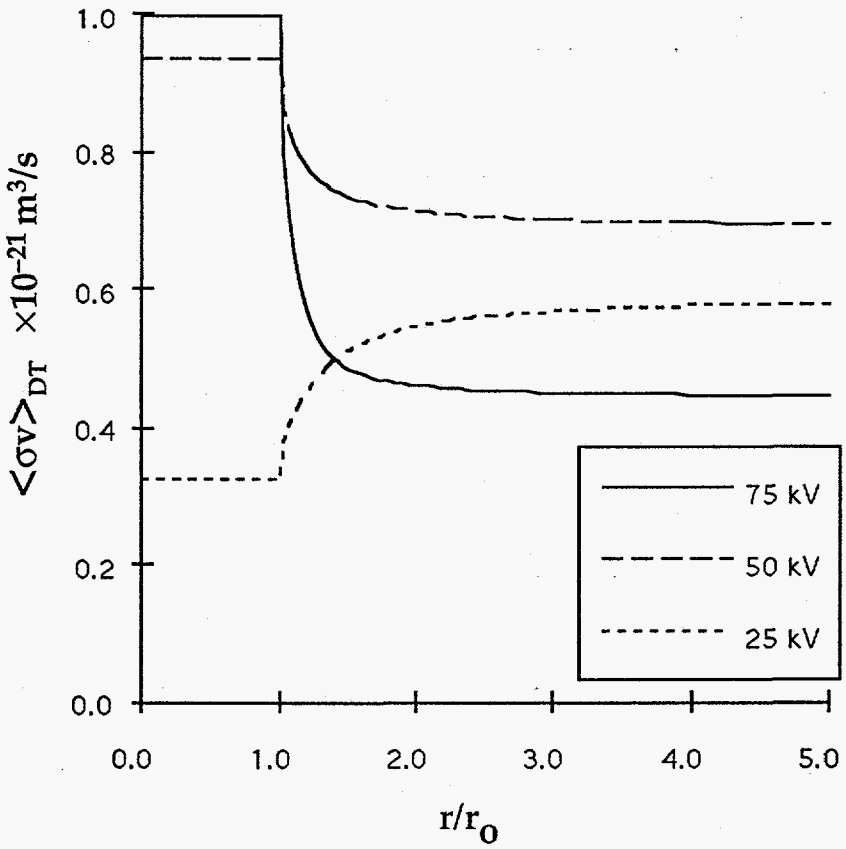

Figure 3. The radial variation of $\langle\sigma v\rangle_{DT}$ for an ion with zero angular momentum is plotted vs. radius for three potential well depths, ϕ_o = 25 kV, 50 kV, and 75 kV. The integral over collision angle was evaluated numerically using fusion cross-sections from Bosch and Hale.

There is significant variation in $\langle\sigma v\rangle_{DT}$ with both radius and potential well depth. The rate coefficient in the core ($r \le r_o$) is that of an isotropic, mono-energetic distribution, as previously evaluated in this context by Miley et al.,[14] and Santarius et al.[15] In the bulk region ($r_o < r < a$) the rate coefficient rapidly approaches that of two counter-streaming beams as considered by Bussard.[10]

In evaluating the total fusion power one should integrate over the angular distributions of both incident ions. The rate coefficient shown in Fig. 3 is averaged only over the angular distribution of one of the incident ions. However, it reproduces the correct result for $r \le r_o$ (where both distributions are isotropic), and for $r \gtrsim 2r_o$, where the dominant contribution to the rate coefficient comes from counter-streaming ions. Hence, only a small error is introduced by

[14]G.H. Miley, J. Nadler, T. Hochberg, Y. Gu, O. Barnouin, and J. Lovberg, Fusion Technology **19**, 840 (1991).

[15]J.F. Santarius, K.H. Simmons, and G.A. Emmert, Bull. Am. Phys. Soc. 39, 1740 (1994).

replacing this second angular average with its value for $L^2=0$. Using this approximation, we have evaluated the effective rate coefficient, as defined in Eq. (22) as a function of the potential well depth for both DT and D-^{3}He reactions. These results are displayed in Fig. 4.

Figure 4. Dependence of $\langle\sigma v\rangle_{DT}^{eff}$ and $\langle\sigma v\rangle_{DHe}^{eff}$ on Potential Well Depth

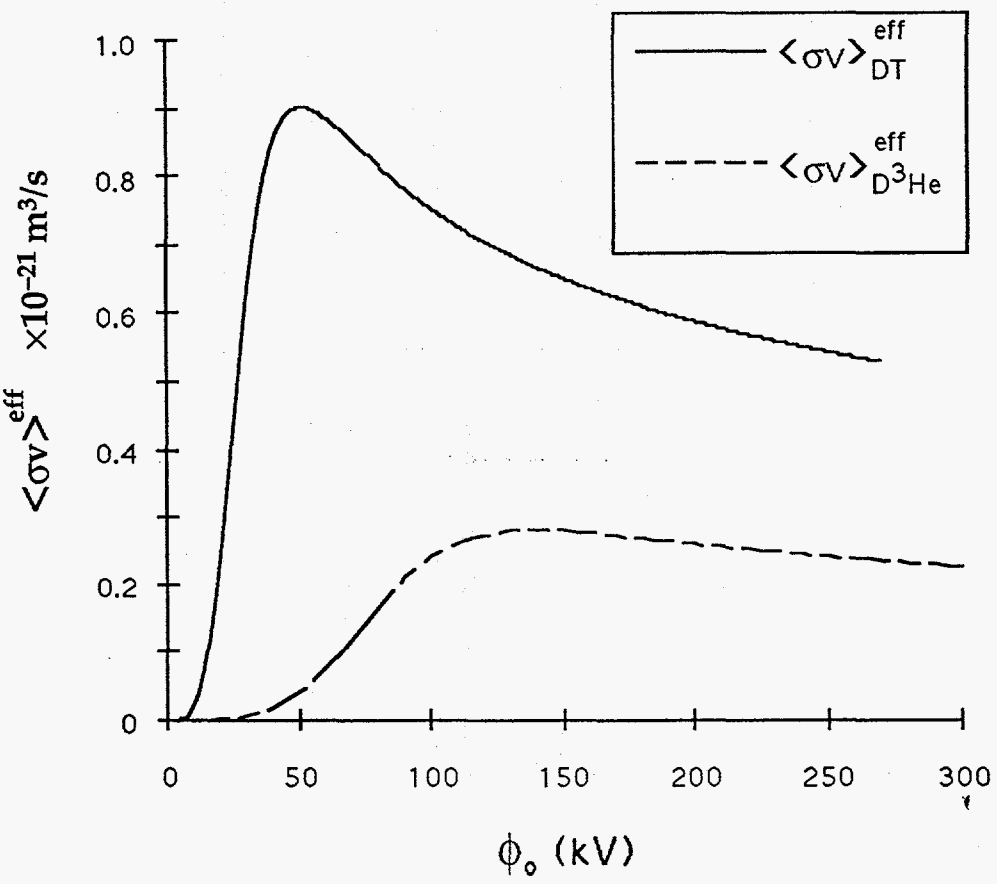

Figure 4. Effective fusion rate coefficient for DT and D^{3}He reactions vs. potential well depth, ϕ_o. The kinetic energy of all particles is taken as $q\phi_o$.

In computing the effective rate coefficients, $\langle\sigma v\rangle_{ss'}^{eff}$, displayed in Fig. 4 we have assumed that the kinetic energy of the incident ions "s" and "s' " are given by $q_s\phi_o$ and $q_{s'}\phi_o$ respectively because we find no advantage in choosing the energy of the heavier ion to be smaller than that of the lighter ion by the ion mass ratio. This ordering of the ion energies was recommended in Ref. 10 as a means of minimizing the energy diffusion resulting from collisions in the "bulk" region, $r_o < r < a$. This issue is discussed further in Sec. 4.

Finally, we compare the effective DT fusion rate coefficients for a mono-energetic IEC system to the Maxwellian averaged rate coefficients in Fig. 5.

Figure 5. Averaged Fusion Rate Coefficients

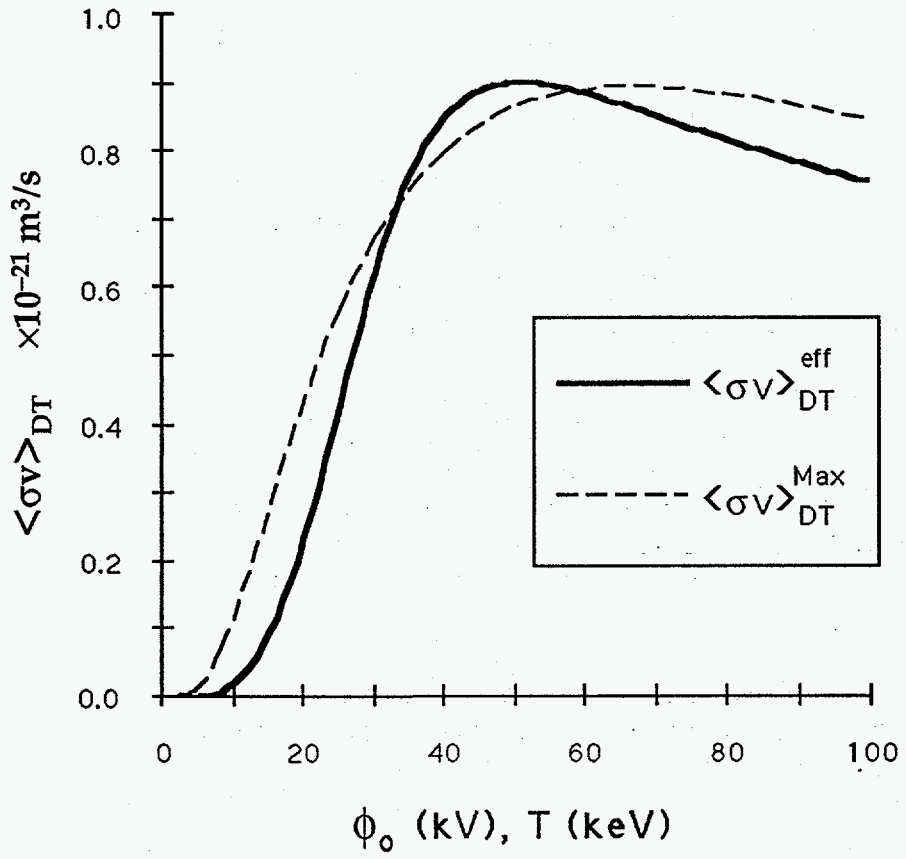

Figure 5. Averaged DT fusion rate coefficients for a mono-energetic IEC distribution (solid line) and for a Maxwellian distribution (dashed line).

The Maxwellian-averaged DT fusion rate coefficient was computed following Bosch and Hale.[13] The mono-energetic IEC rate coefficient $\langle\sigma v\rangle_{DT}^{eff}$ has a peak value of 0.90×10^{-21} m^3/s at a potential well depth ϕ_o=50.7 kV; while the Maxwellian averaged fusion rate coefficient $\langle\sigma v\rangle_{DT}^{Max}$ has a peak value of 0.89×10^{-21} m^3/s at an ion temperature of 75.0 keV. We see that, despite claims to the contrary,[10] the averaged rate coefficient for a mono-energetic IEC system is not significantly greater than the Maxwellian-averaged fusion rate coefficient at similar energies. In fact, the only significant qualitative difference between these averaged rate coefficients is that $\langle\sigma v\rangle_{DT}^{eff}$ goes to zero more rapidly at small ϕ_o

than does $\langle\sigma v\rangle_{DT}^{Max}$ at small T_i. Hence, if it proves difficult to achieve mean ion energies above 20–30 keV, then thermal ion distributions are superior to mono-energetic IEC distributions because they have a higher reactivity.

The Maxwellian-averaged D^3He rate coefficient, $\langle\sigma v\rangle_{D^3He}^{Max}$, may also be compared to the corresponding mono-energetic IEC rate coefficient, $\langle\sigma v\rangle_{D^3He}^{eff}$. The peak value of the mono-energetic rate coefficient occurs at ϕ_o = 140 kV, where it takes the value $\langle\sigma v\rangle_{D^3He}^{eff} = 2.8\times10^{-22}m^3/s$. A direct comparison with the Maxwellian averaged D^3He rate coefficient of Bosch and Hale is not possible because their parameterization of $\langle\sigma v\rangle_{D^3He}^{Max}$ is valid only for $T_i \leq 190$ keV. However, Miley[16] reports a maximum value in the Maxwellian-averaged D^3He rate coefficient, $\langle\sigma v\rangle_{D^3He}^{Max} = 2.5\times10^{-22}m^3/s$ at T_i = 250 keV. The somewhat larger difference (about 11%) between these averaged rate coefficients is similar in magnitude to the change in the magnitude of the D^3He rate coefficient associated with the improved parameterization of the fusion cross-section developed by Bosch and Hale (see Fig. 22 of Ref. 13). However, the peak value of the effective IEC rate coefficient for D^3He is not significantly larger than that of the corresponding Maxwellian averaged rate coefficient.

We conclude that significant increases in the power density of an IEC system relative to other confinement systems result only from the choice of a higher mean ion energy at the projected operating point and from the strong central peaking of the ion density associated with the anisotropic ion distribution function assumed by proponents of IEC systems.

[16]G.H. Miley, H. Towner, N. Ivich, "Fusion Cross Sections and Reactivities", U. of Ill. Report C00-2218-17 (June, 1974).

4. Collisional Relaxation of the Ion Distribution Function

The strong focusing of ions at the center of the well is the defining feature of IEC systems. This focusing leads to a substantial enhancement of the total fusion power at fixed stored energy. The total fusion power within our square-well model,

$$P_{fusion} = \frac{1}{4} Y_{DT} \int d^3r \; n_i^2(r) \langle \sigma v \rangle_{DT} (r)$$

$$\approx \frac{8}{9} \frac{a}{r_o} \left(\frac{\langle n_i \rangle_{Vol}}{2} \right)^2 V \; Y_{DT} \; \langle \sigma v \rangle_{DT}^{eff} ,$$

is enhanced relative to what would be obtained with an isotropic ion distribution function $\left(\text{for which } n_i = \langle n_i \rangle_{Vol}\right)$ by the factor $\frac{8}{9} \frac{a}{r_o}$. This enhancement results from the central peaking of the ion density which, in turn, depends critically on maintaining a strong anisotropy in the ion distribution function [i.e., insuring that $f_s(\varepsilon, L^2)$ goes to zero rapidly for $L^2 > (m_s v_s r_o)^2$]. Hence, it is important to examine effects which will tend to reduce this anisotropy in the ion distribution function.

Ion-ion collisions are an obvious mechanism for reducing the ion anisotropy. It follows from the Boltzmann H-theorem that ion-ion collisions will drive the system to an equilibrium in which $f_s(\varepsilon, L^2) \sim \exp(-\varepsilon/T)$, that is, to a state in which there is no ion anisotropy and the only variation in the ion density arises from variations in the potential, such that $n_s(r) \sim \exp(-q_s\phi(r)/T)$. If the ion distribution function is allowed to relax to thermal equilibrium, the key advantage of IEC systems (enhanced fusion power at fixed stored energy due to strong density peaking) is lost. However, ion collision rates are low (of the order of 1 Hz) at the energy and densities projected for IEC reactors. Hence, the power required to maintain a non-equilibrium ion distribution function might be less than the fusion power produced. In order to investigate this possibility we must first evaluate the collisional relaxation rates of the ion distribution function.

A. Collisional Relaxation of Ion Anisotropy.

Coulomb collisions will result in an increase in $\langle L^2 \rangle$ due to transverse scattering (that is, scattering of the ion velocity so that it has a component in the plane perpendicular to $\hat{\mathbf{e}}_r$). In Appendix A we show that, in the limit $L^2 \rightarrow 0$ (so that the ion velocity is nearly radial over most of its orbit), the collisional rate of increase in the mean-square transverse velocity for ions of species s and speed

$$v_s \equiv \sqrt{\frac{2q_s\phi_o}{m_s}} \tag{27}$$

is given by

$$\frac{d}{dt} <\Delta v_\perp{}^2> \; = \; 2v_s{}^2 \sum_{s'} \nu_o^{s/s'} \; u_{s'} \; I_\perp(\mu_o, u_{s'}) \, , \tag{28}$$

where

$$u_{s'} \equiv \frac{v_s}{v_{s'}} \, , \tag{29}$$

following Book,[17] we have defined

$$\nu_o^{s/s'} \equiv \frac{4\pi q_s{}^2 q_{s'}{}^2 n_{s'} \, \mathrm{Ln} \, \Lambda_{ss'}}{m_s{}^2 v_s{}^3} \, , \tag{29}$$

and

$$\mu_o \; = \; \begin{cases} 0 & r \le r_o \\ \sqrt{1 - r_o{}^2/r^2} & r > r_o \end{cases} \tag{30}$$

is the cosine of the angle between $\mathbf{v}$ and $\hat{\mathbf{e}}_r$ at which the model IEC distribution function goes to zero at a given radius.

[17]D.L. Book, *NRL Plamsa Formulary,* NRL Publication 0084-4040 (NRL, Washington DC, 1986). See page 31.

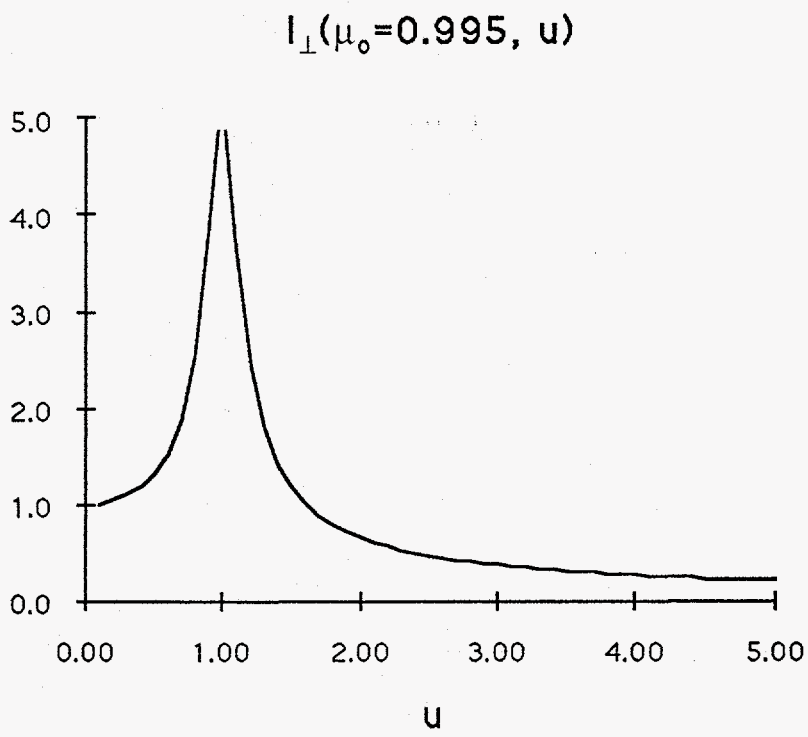

Figure 6. $I_\perp(\mu_o, u)$ is displayed as a function of test-particle speed (u) for $\mu_o = 0.995$ (corresponding to $r = 10\ r_o$). The resonance at u=1 results from self-collisions among co-moving particles.

The variation of the collision integral $I_\perp(\mu_o,u)$ with particle speed is shown in Fig. 6 for a typical location in the plasma bulk, $r = 10\ r_o$. At each location in this region ($r_o < r \leq a$) the ion distribution resembles two counter-streaming beams [see Eq. (23)]. The resonance at u=1 (corresponding to $v_s=v_{s'}$) in Figure 6 describes collisions between particles which are co-moving in the same beam. Collisions between co-moving particles leads to strong coupling between the transverse and longitudinal velocity dispersion of these beams as pointed out by Rosenberg and Krall.[12] We will return to this important effect in Sec. 5. In this section we will ignore the internal structure of these beams, focusing on the rate of increase in velocity dispersion due to collisions between ions in counter-streaming beams. We can remove the effect of collisions between co-moving particles from our representation of the collision integral by replacing the collision integral $I_\perp(\mu_o, u)$ with $I'_\perp(\mu_o, u)$, which has been cut-off at $\mu_c = 0.95$ to eliminate the effect of collisions between co-moving particles in the bulk plasma as described in Appendix A. In the bulk region (where $\mu_o \equiv \sqrt{1-(r_o/r)^2} \approx 1$) this modified collision integral is well approximated by

$$\lim_{\mu_o \to 1} \left[I'_\perp(\mu_o, u)\right] = \frac{1}{2}\,\frac{1}{u_{s'}+1}\ . \tag{31}$$

The variation of $I'_{\perp}(\mu_o, u)$ with particle speed in the plasma core ($r \le r_o$) is shown in Fig. 7.

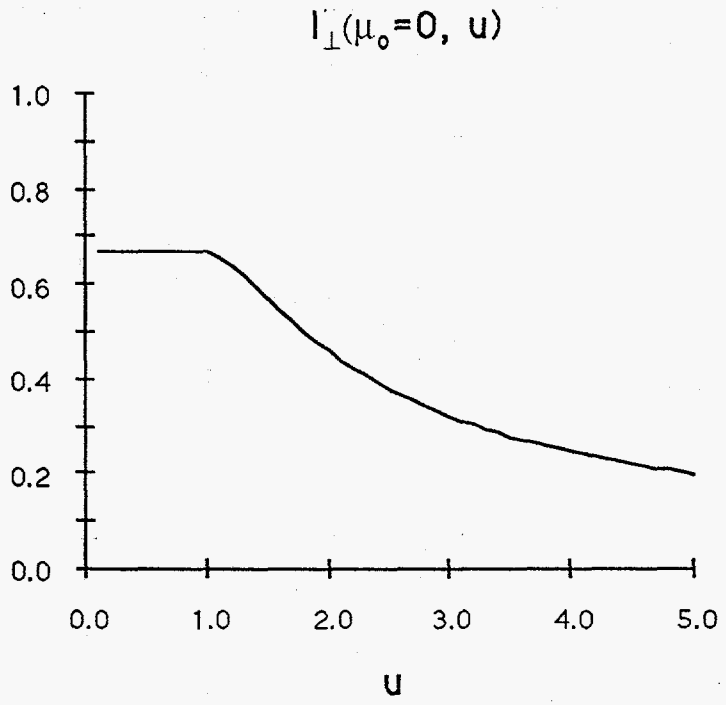

Figure 7. $I_{\perp}(\mu_o, u)$ is displayed as a function of test particle speed for $\mu_o=0$, corresponding to radial locations in the plasma core, $r \le r_o$.

At a given radius the collisional rate of increase in L^2 is simply related to the collisional rate of increase in the transverse velocity dispersion,

$$\left.\frac{dL^2}{dt}\right|_{\text{collisions}} = m_s^2 r^2 \frac{d}{dt} \langle \Delta v_{\perp}^2 \rangle . \qquad (32)$$

The rate of increase in L^2 varies over the ion orbit. However, at the ion densities and energies projected for an IEC reactor the change in L^2 due to collisions during a single orbit is small. Hence, we average the collisional change in L^2 over the ion orbit to eliminate the rapid time scale associated with ion orbital motion, and obtain the bounce-averaged rate of change in L^2 :

$$\left\langle \frac{d}{dt} L^2 \right\rangle_{\text{collisions}} = \frac{1}{\tau_b} \int_0^a \frac{dr}{v_r} \left.\frac{dL^2}{dt}\right|_{\text{collisions}} . \qquad (33)$$

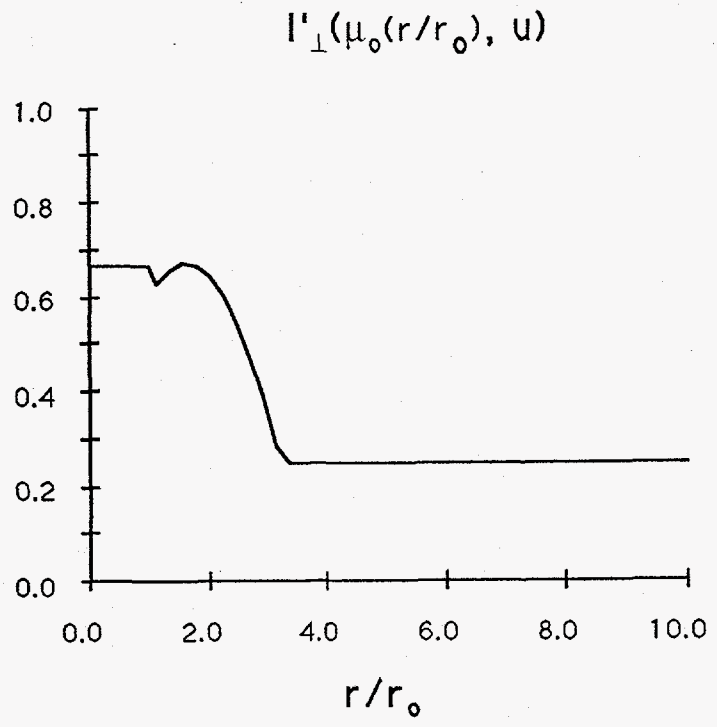

Figure 8. Radial variation in the transverse collision integral, $I'_{\perp}(\mu_o(r), u)$ is displayed for a test particle with speed u=1. The structure at $r/r_o \approx 1$ is associated with the cut-off in $I'_{\perp}$ at $\mu_c=0.95$ applied for $r/r_o \geq 1$.

The radial dependence of the transverse collision integral, $I'_{\perp}(\mu_o(r), u)$ is shown in Fig. 8. Except for a small region about the plasma core ($r \lesssim 3r_o$), $I'_{\perp}$ is well approximated by Eq. (31). Hence, the rate of increase in the transverse velocity dispersion depends on radius mainly through the ion density. We may isolate this dependence by multiplying and dividing by the ion density, and noting that the factor, $(\nu_o^{s/s'}/n_s)$ is nearly independent of radius. Hence, we may approximate the bounce-average collisional rate increase in L^2 for ions of species s as

$$\frac{d}{dt}\langle L^2\rangle_{collisions} \approx m_s^2 v_s^2 \sum_{s'} \frac{\nu_o^{s/s'}}{n_{s'}} \frac{v_s}{v_s + v_{s'}} \int_0^a \frac{dr}{a} r^2 n_{s'}(r) \qquad (34)$$

$$\approx c_s L_a^2 \langle n_s\rangle_{Vol} \left(\frac{\nu_o^{s/s}}{n_s}\right) \approx c_s L_a^2 \langle \nu_o^{s/s}\rangle_{Vol} \qquad (35)$$

where

$$c_s \equiv \sum_{s'} \frac{v_s}{v_s + v_{s'}} \tag{36}$$

and

$$L_a^2 = \frac{2}{3}(m_s v_s a)^2 \tag{37}$$

is the value of $<L^2>$ for an isotropic, mono-energetic ion distribution—that is, an ion distribution that yields a constant ion density throughout the trap. For a DT plasma we find

$$c_d = \frac{1}{2} + \frac{1}{1 + \sqrt{m_d/m_t}} \approx 1.051, \tag{38}$$

and

$$c_t = \frac{1}{2} + \frac{1}{1 + \sqrt{m_t/m_d}} \approx 0.949. \tag{39}$$

We were motivated to introduced the volume average scattering rate,

$$<\nu_o^{s/s'}>_{Vol} \equiv \frac{4\pi q_s^2 q_{s'}^2 \, \mathrm{Ln}\, \Lambda_{ss'}}{m_s^2 v_s^3} <n_{s'}>_{Vol} \tag{40}$$

because (assuming that the total number of ions is conserved) this rate is constant as the ion distribution function relaxes towards isotropy. It follows that the rate of increase in $<L^2>$ is independent of time and that, even after taking credit for the central concentration of the ion density, the ion distribution function relaxes to isotropy in a time[18]

$$\tau_L^s \approx \frac{1}{c_s <\nu_o^{s/s}>_{Vol}} \, . \tag{41}$$

For the reference IEC reactor of Table I this works out to $\tau_L^d \approx 0.43$ s.

[18]The 2-D analogue of this calculation applies to systems with rotational symmetry like the MIGMA. Here ion focussing results from the constancy of the canonical angular momentum while that the ion density fall with radius as 1/r. Hence, off-axis collisions will again cause a loss of the ion focus on the (volume-averaged) ion collisional time scale.

If at t=0 we prepare an IEC trap with a well-focused ion distribution, the collisional increase in $\langle L^2 \rangle$ will result in a spreading of the radius of the ion focus with time. If we constrain the ion distribution to maintain the form defined in Sec. 2, and evaluate L_o at each instant in time such that $\langle L^2 \rangle$ increases at collisional rate, the radius of the ion focus will be given by

$$r_o(t) \approx a \sqrt{c_s \langle \nu_o^{s/s} \rangle_{Vol} \, t} \quad . \tag{42}$$

Note that, while the focus expands until the focal radius, $r_o \approx a$ and the ion distribution is fully isotropic in time τ_i^s, the instantaneous rate of increase in the focal radius,

$$\frac{1}{r_o} \frac{dr_o}{dt} \approx \frac{c_s}{2} \left(\frac{a}{r_o} \right)^2 \langle \nu_o^{s/s} \rangle_{Vol}$$

is much faster.

In the absence of particle sources and sinks, collisional effects define a minimum rate of at which the ion focus degrades. The actual rate of can be substantially higher. For example, asymmetries in the confining potential may occur due to the inherent lack of symmetry in the magnetic fields needed to confine the electrons that generate the potential well,[19] asymmetries associated internal or external electrodes, asymmetries associated with the apparatus that injects the ions into the trap, or due to waves and instabilities.[20] Even very small asymmetries in the confining potential can substantially increase the rate at which the ion distribution function relaxes towards isotropy because they scatter longitudinal velocity into transverse velocity at a radius $r \approx a$ (so for a fixed $\Delta v_\perp^2$ we generate the maximum change in L^2); and because a "collision" occurs between each ion and the confining potential once each bounce period. Hence, we may estimate the rate of change in L^2 due to asymmetries in the confining potential as

$$\frac{d}{dt} \langle L^2 \rangle_{\text{asymmetries}} \sim m \left(\frac{\delta\phi}{\phi_o} \right) \frac{1}{\tau_b} \quad , \tag{43}$$

where "m" is the mode number and $\delta\phi$ is the magnitude of the asymmetry in the confining potential.

---

[19] T.J. Dolan, Fusion Technology 24, 128 (1993).

[20] See, e.g., C.W. Barnes, Ann. N.Y. Acad. Sci. 251, 370 (1975); S.K. Wong and N.A. Krall, Physics of Fluids B 5, 1706 (1993).

For the 50 keV deuterons in the reference IEC reactor described in Table I, $1/\tau_b \approx 1.1$ MHz, while $\langle \nu_o^{d/d} \rangle_{Vol} \approx 2.23$ Hz. Hence, the bounce frequency is larger than the collisional rate of isotropization by a factor of 5×10^5. Clearly, even very small asymmetries in the confining potential can lead to relaxation of the anisotropy in the ion distribution function at a faster rate than Coulomb collisions.

B. Collisional Relaxation of the Ion Energy Distribution.

Despite the absence of any significant advantage in fusion reactivity or direct impact on ion focusing, it is still important to examine the collisional relaxation of the mono-energetic ion energy distribution function because the energy dependence of the distribution function is important in determining the equilibrium potential; and the rate of thermalization in energy has important implications regarding the effect of collisions between co-moving ions on the evolution of the ion anisotropy (see Sec. 5).

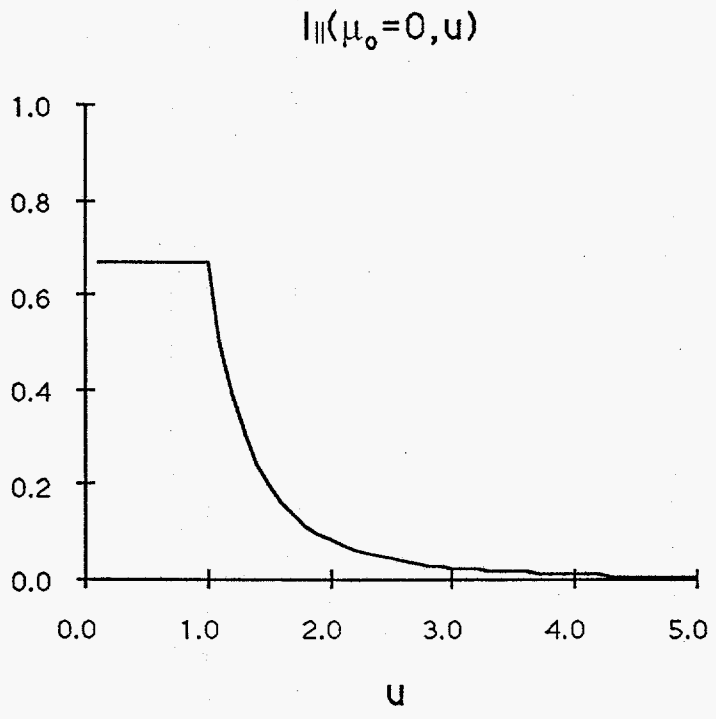

Figure 9. $I_{||}(\mu_o, u)$ is displayed as a function of test particle speed for $\mu_o=0$, corresponding to radial locations in the plasma core, $r \le r_o$.

In Appendix A it is shown that the collisional rate of increase in the longitudinal velocity dispersion of ions of species "s" is given by

$$\frac{d}{dt} <\Delta v_{\|}^2>_s = \sum_{s'} \nu_o^{s/s'} v_s^2 \frac{v_s}{v_{s'}} I_{\|}(\mu_o, u_{s'}) . \qquad (44)$$

The variation of the longitudinal collision integral with speed in the plasma core ($r \le r_o$), is shown in Fig. 9. For $u \le 1$, $I_{\|}(\mu_o=0, u)$ takes the same value (2/3) as the transverse collision integral, $I_{\perp}(\mu_o=0, u)$. Hence, the collisional diffusion is isotropic in the core at low ion velocity (as expected for an isotropic distribution function), while pitch angle scattering (and drag, which is not treated here) are the dominant collisional effects for fast particles.

Unlike the transverse collision integral, the longitudinal collision integral approaches zero in the bulk region ($r > r_o$), where it may be approximated by

$$I'_{\|}(\mu_o(r), u) \approx \frac{1}{4} \frac{(r_o/r)^2}{(1 + u_{s'})^3} \qquad (r >> r_o) . \qquad (45)$$

Bussard[10] first noted that bulk collisions would not cause energy diffusion. However, Bussard based his conclusion on an additional requirement—that the ion energies be chosen such that the energy of the heavier ion is smaller than that of the lighter ion by the ratio of the ion masses. When this condition is satisfied the center-of-mass frame for collisions between counter-streaming ions in the plasma bulk is nearly identical to the lab frame. We obtain this same result more generally, concluding that collisions in the bulk plasma do not cause energy diffusion for any choice of the relative ion energies. Hence, the result is not a consequence of the kinematics of two-body collisions in the center-of-mass frame since, for general relative energies of the two ion species, the center-of-mass and lab frames of reference are not identical. Rather, it follows from the assumption that the scattering angle is small (which is always the case for the dominant contribution to the Coulomb collision operator) together with the fact that, in the bulk plasma region, the velocities of the colliding particles are nearly co-linear. For small-angle collisions the momentum transfer between the colliding particles can be obtained by treating the interaction as a perturbation, and integrating along the unperturbed (i.e., parallel, straight-line) orbits. When the impact parameter is finite (as required for small angle collisions) it is easily seen that the momentum transfer (the time integral of the force on one particle due to interaction with the other particle) must be perpendicular to the particle velocities for any central force law. Hence, bulk collisions can produce pitch-angle scattering (as described by the transverse collision integral) but not energy diffusion. This conclusion holds independent of the relative energy of the colliding ions. We conclude that only the plasma core contributes to the

collisional increase in the longitudinal velocity dispersion. This is apparent in Fig. 10, which shows the radial dependence of $I'_{\|}(\mu_o, u)$.

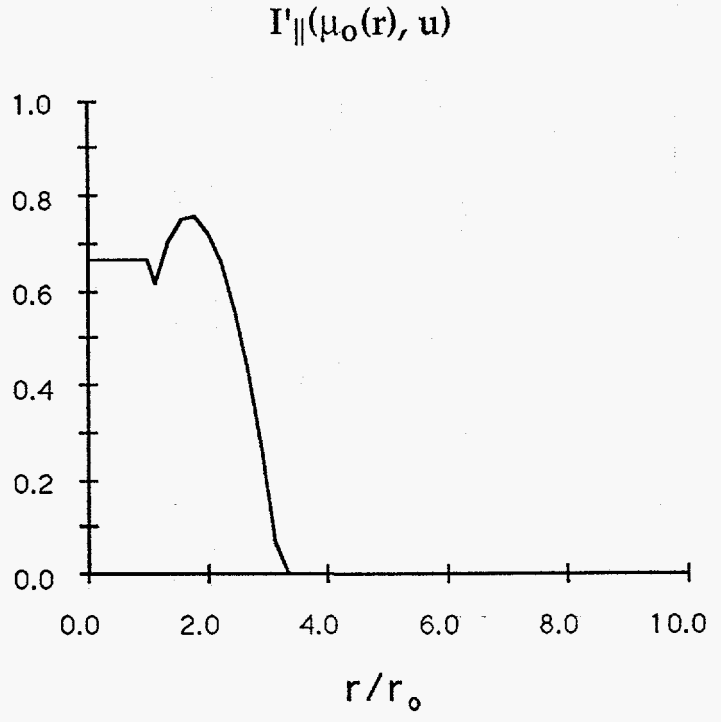

Figure 10. Radial variation in the logitudinal collision integral, $I'_{\|}(\mu_o(r), u)$ is displayed for a test particle with speed u=1. The structure at $r/r_o \approx 1$ is associated with the cut-off in $I'_{\|}$ at $\mu_c = 0.95$ applied for $r/r_o \geq 1$.

The bounce averaged collisional rate of increase in the ion energy is given by

$$\langle \nu_\varepsilon^s \rangle_{orbit} = \frac{1}{v_s^2} \frac{d}{dt} \langle \Delta v_{\|}^2 \rangle_s \qquad (46)$$

$$\approx \sum_{s'} \frac{\nu_o^{s/s'}}{n_{s'}} \frac{v_s}{v_{s'}} \int_0^a \frac{dr}{a} \; n_{s'}(r) \, I_{\|}(\mu_o(r), u_{s'}))$$

$$\approx \frac{2}{3} d_s \left(\frac{a}{r_o}\right) \langle \nu_o^{s/s} \rangle_{Vol} , \qquad (47)$$

where

$$d_s = \sum_{s'} \frac{v_s}{v_{s'}} \int_0^a \frac{dr}{a} \frac{n_{s'}(r)}{n_{s0}} I_{||}(\mu_0(r), v_s/v_{s'}) . \qquad (48)$$

We have computed the orbit integral numerically for a DT plasma with equal deuterium and tritium fractions, finding

$$d_d \approx 1.73 \qquad (49)$$

and

$$d_t \approx 1.91 . \qquad (50)$$

At constant ion convergence ratio (a/r_0), the ion energy distribution relaxes to a Maxwellian in a time of order

$$\tau_\varepsilon^s \approx \frac{3}{2d_s} \left(\frac{r_0}{a}\right) \frac{1}{\langle \nu_0^{s/s} \rangle_{Vol}} << \tau_L^s . \qquad (51)$$

For our reference IEC reactor of Table I this works out to $\tau_\varepsilon^d \approx 5.4$ ms. Given this relatively rapid rate of ion thermalization, it is clear that it is at least as difficult to maintain the mono-energetic character of the IEC ion distribution function as it is to maintain the anisotropy required for central focusing of the fuel ions. One must question the strategy of attempting to maintain a (nearly) mono-energetic ion distribution function, and consider allowing the ion distribution to relax to a Maxwellian in energy, while retaining the anisotropy. We will return to this question in Section 6.

5. Collisions Between Co-Moving ions

When mapped to radial locations in the bulk plasma ($r_o < r < a$) the model IEC ion distribution function of section 2 yields a local ion distribution that corresponds to two ion beams counter-streaming at speeds $\pm v_s$ [see Eq. (23)]. In this section we consider the effect of collisions between ions in the same beam (that is, co-moving ions) on the longitudinal and transverse velocity dispersion of that beam. In earlier work, Rosenberg and Krall[12] considered the collisional evolution of the ion distribution function in a model in which the confining potential has a finite gradient at the plasma surface. They point out that, for a nearly mono-energetic ion distribution function, the mean-squared ion velocity near the ion injection point (which is simply related to the longitudinal and transverse velocity dispersion discussed in section 4) is small compared to ion streaming velocity, v_s. Hence, the ion collision frequency, which goes as $1/v^3$, will be large at the plasma surface. Rosenberg and Krall conclude that these edge collisions cause a relaxation of the longitudinal and transverse velocity dispersion towards isotropy ($\langle \Delta v_\perp^2 \rangle_s \approx 2 \langle \Delta v_\parallel^2 \rangle_s$) at a rate

$$\left.\frac{d\langle \Delta v^2 \rangle}{dt}\right|_{\text{edge collisions}} \sim \frac{r_\phi}{a} \sqrt{\frac{q_s \phi_o}{m\langle \Delta v^2 \rangle}}\, q_s \phi_o \left\langle \nu_o^{s/s} \right\rangle_{\text{vol}} \qquad (52)$$

where

$$r_\phi \equiv \left(\frac{1}{\phi_o} \left.\frac{d\phi}{dr}\right|_{r=a} \right)^{-1} \qquad (53)$$

is the potential gradient scale length at $r \approx a$. The effect of these edge collisions is to transfer energy between the longitudinal and transverse degrees of freedom. That is, to couple the energy spread of the ion beam to the quality of the ion focus.

Edge collisions are omitted from our square-well model because r_ϕ vanishes for a square well. However, collisions between co-moving ions in the plasma bulk have the same effect—i.e., these collisions couple the longitudinal and transverse degrees of freedom, the collisional rate is large because the relative velocity of the co-moving ions is small, and they act over most of the ion orbit, rather than just at the plasma surface. Collisions between co-moving ions change the beam velocity dispersion at a rate

$$\left.\frac{d\langle \Delta v^2 \rangle}{dt}\right|_{\text{co-moving ions}} \sim \sqrt{\frac{q_s \phi_o}{m\langle \Delta v^2 \rangle}}\, q_s \phi_o \left\langle \nu_o^{s/s} \right\rangle_{\text{vol}}. \qquad (54)$$

Since r_ϕ/a is expected to be less than one, we conclude that bulk collisions between co-moving ions dominate the edge collisions emphasized in Ref. 12. These collisions are included in our square-well model, and will be examined in detail in the remainder of this section.

Following Rosenberg and Krall, we resolve the singularity associated with the delta function in the ion distribution function by modeling the internal structure of the beam-like ion distribution function in the plasma bulk by assuming that it is drifting bi-Maxwellian. The longitudinal and transverse temperatures of the beam are chosen to reproduce the longitudinal and transverse velocity dispersion discussed in section 4. The ion distribution function has a longitudinal velocity dispersion

$$<\Delta v_\parallel^2> \equiv \frac{T_\parallel^{(s)}}{m_s} \tag{55}$$

and a transverse velocity dispersion

$$<\Delta v_\perp^2>(r) = \frac{<L^2>}{m_s^2 r^2} \equiv \frac{2T_\perp^{(s)}(r)}{m_s}. \tag{56}$$

Note that the transverse velocity dispersion of the beam, $<\Delta v_\perp^2>$, and the transverse temperature, $T_\perp^{(s)}$, are simply related to the ion focal radius, r_o [see Eq. (57) below]. Hence, we only introduce one new parameter, $T_\parallel^{(s)}$, to describe the internal structure of the counter-streaming ion beams.

The transverse temperature, $T_\perp^{(s)}$, is strong functions of radius. This strong radial variation in $T_\perp^{(s)}$ results from the fact that different groups of ion orbits intersect at each radial location. Hence, we find it convenient to compute the contribution of collisions among co-moving ions to the transverse velocity dispersion of the ion "beam" by relating it to $d<L^2>/dt$. We may then compute the local value of $T_\perp^{(s)}(r)$ and the ion focal radius from the relations

$$T_\perp^{(s)}(r) = T_\perp^{(s)}(a)\frac{a^2}{r^2} = \frac{1}{2} q_s\phi_o \frac{r_o^2}{r^2} = \frac{<L^2>}{2m_s r^2}. \tag{57}$$

In the absence of collisions between co-moving ions the velocity dispersion would increase at the (bounce-averaged) rates computed in section 4.

These rates of increase in the beam longitudinal temperature and $\langle L^2 \rangle$ for ions of species s are

$$\left.\frac{dT_{\|}^{(s)}}{dt}\right|_{\text{core collisions}} = m_s \frac{d}{dt} \langle \Delta v_{\|}^2 \rangle \tag{58}$$

$$\approx \frac{4}{3} d_s \left(\frac{a}{r_o}\right) q_s \phi_o \langle \nu_o^{s/s} \rangle_{Vol} \tag{59}$$

and

$$\left.\frac{d\langle L^2 \rangle}{dt}\right|_{\text{bulk collisions}} \approx c_s L_a^2 \langle \nu_o^{s/s} \rangle_{Vol} , \tag{60}$$

or, equivalently,

$$\left.\frac{d}{dt}\left(\frac{r_o}{a}\right)\right|_{\text{bulk collisions}} \approx \frac{2}{3} c_s \left(\frac{a}{r_o}\right) \langle \nu_o^{s/s} \rangle_{Vol} . \tag{61}$$

A. Nearly Mono-Energetic Ions, $\frac{T_{\|}^{(s)}}{q_s \phi_o} < \frac{1}{2} \frac{r_o^2}{a^2}$

We follow Kogan[21] in computing the collisional relaxation of the beam velocity dispersion between the longitudinal and transverse degrees of freedom. In the spirit of the model IEC ion distribution function of section 2, we begin by considering a beam with a finite ion convergence radius (so that $\langle L^2 \rangle > 0$) and a nearly mono-energetic ion distribution function, such that $T_{\perp}^{(s)}(a) \geq T_{\|}^{(s)}$ or, equivalently, $T_{\|}^{(s)}/q_s\phi_o < 0.5\, r_o^2/a^2$. Then $T_{\perp}^{(s)} \geq T_{\|}^{(s)}$ everywhere in the well, and the local rates of change in $T_{\perp}^{(s)}$ and $T_{\|}^{(s)}$ due to collisions among co-moving ions are[21]

$$\left.\frac{dT_{\|}^{(s)}}{dt}\right|_{\text{co-moving ions}} \approx \sqrt{\pi} \left(\frac{r}{r_o}\right) q_s \phi_o \, \nu_o^{s/s} \tag{62}$$

---

[21] V.I. Kogan, in *Plasma Physics and the Problem of Controlled Thermonuclear Reactions* (Pergammon Press, New York, 1961), Vol. 1, p. 153.

and

$$\left.\frac{dT_{\perp}^{(s)}}{dt}\right|_{\text{co-moving ions}} \approx -\frac{1}{2}\sqrt{\pi}\left(\frac{r}{r_o}\right) q_s \phi_o \, \nu_o^{s/s}. \tag{63}$$

It follows that the local rate-of-change in $\langle L^2 \rangle$ due to collisions among co-moving ions is

$$\left.\frac{d\langle L^2\rangle}{dt}\right|_{\text{co-moving ions}} \approx -\frac{3}{4}\sqrt{\pi}\left(\frac{r^3}{a^2 r_o}\right) L_a^2 \, \nu_o^{s/s}. \tag{64}$$

These rates need to be averaged over that portion of the ion trajectory with $r \gtrsim r_c$, where

$$r_c \equiv \frac{r_o}{\sqrt{1-\mu_c^2}} \approx 3.20\, r_o \tag{65}$$

is the radius at which the cut-off in the longitudinal collisional integrals introduced in section 4 to remove the effect of collisions among co-moving ions becomes effective; and we have again taken $\mu_c \approx 0.95$. The orbit-averaged rates are

$$\left.\frac{dT_{\parallel}^{(s)}}{dt}\right|_{\text{co-moving ions}} \approx \frac{\sqrt{\pi}}{4}\,\text{Ln}\left(\frac{a}{r_c}\right) \times \frac{4}{3}\left(\frac{a}{r_o}\right) q_s \phi_o \, \langle \nu_o^{s/s} \rangle_{\text{Vol}} \tag{66}$$

and

$$\left.\frac{d\langle L^2\rangle}{dt}\right|_{\text{co-moving ions}} \approx -\frac{\sqrt{\pi}}{8}\left(\frac{a}{r_o}\right)\left(1-\frac{r_c^2}{a^2}\right) \times L_a^2 \, \langle \nu_o^{s/s} \rangle_{\text{vol}}, \tag{67}$$

or, equivalently,

$$\left.\frac{d}{dt}\left(\frac{r_o}{a}\right)\right|_{\text{co-moving ions}} \approx -\frac{\sqrt{\pi}}{12}\left(\frac{a}{r_o}\right)^2\left(1-\frac{r_c^2}{a^2}\right)\langle \nu_o^{s/s} \rangle_{\text{vol}}. \tag{68}$$

Both core collisions and collisions among co-moving ions lead to an increase in the longitudinal velocity dispersion. However, even for a relatively poorly focused ion distribution,

$$\frac{r_o}{a} < \frac{\sqrt{\pi}}{8c_s} \approx 0.21 , \qquad (69)$$

the decrease in $<L^2>$ due to collisions among co-moving ions will dominate the increase due to collisions in the bulk plasma and $<L^2>$ will decrease. As a result, the ion distribution will rapidly evolve until $T_\perp^{(s)} = T_\parallel^{(s)}$ at r=a.

B. Moderately Thermalized Ion Distributions, $\frac{1}{2}\frac{r_o^2}{a^2} \le \frac{T_\parallel^{(s)}}{q_s\phi_o} \le \frac{1}{2}\frac{r_o^2}{r_c^2}$

We are led to consider the effects of collisions among co-moving ions in the limit that the longitudinal velocity dispersion is large compared to the transverse velocity dispersion, $T_\parallel^{(s)} > T_\perp^{(s)}$. In this limit the local rates of change in $T_\parallel^{(s)}$ and $T_\perp^{(s)}$ due to collisions among co-moving ions are[21]

$$\left.\frac{dT_\parallel^{(s)}}{dt}\right|_{\text{co-moving ions}} \approx -\sqrt{\frac{2}{\pi}}\left(\frac{q_s\phi_o}{T_\parallel^{(s)}}\right)^{1/2} \text{Ln}\left(\frac{8\,T_\parallel^{(s)}}{q_s\phi_o}\frac{r^2}{r_o^2}\right) q_s\phi_o\,\nu_o^{s/s} \qquad (70)$$

and

$$\left.\frac{dT_\perp^{(s)}}{dt}\right|_{\text{co-moving ions}} \approx \sqrt{\frac{1}{2\pi}}\left(\frac{q_s\phi_o}{T_\parallel^{(s)}}\right)^{1/2} \text{Ln}\left(\frac{8\,T_\parallel^{(s)}}{q_s\phi_o}\frac{r^2}{r_o^2}\right) q_s\phi_o\,\nu_o^{s/s} . \qquad (71)$$

It follows that the local rate-of-increase in $<L^2>$ due to collisions among co-moving ions is

$$\left.\frac{d<L^2>}{dt}\right|_{\text{co-moving ions}} \approx \sqrt{\frac{9}{8\pi}}\left(\frac{r^2}{a^2}\right)\left(\frac{q_s\phi_o}{T_\parallel^{(s)}}\right)^{1/2} \text{Ln}\left(\frac{8\,T_\parallel^{(s)}}{q_s\phi_o}\frac{r^2}{r_o^2}\right) L_a^2\,\nu_o^{s/s} . \qquad (72)$$

We perform the orbit average by dividing the ion orbit into a portion at small radius, $r < r_X$, where $T_\perp^{(s)}(r) > T_\parallel^{(s)}$, and a portion at large r, $r > r_X$, where

$T_{\|}^{(s)} > T_{\perp}^{(s)}(r)$, using the expressions for the local rate of change in the longitudinal and transverse temperatures appropriate for each region. The radius $r_\times$, where $T_{\perp}^{(s)}(r_\times) = T_{\|}^{(s)}$, is given by

$$r_\times \equiv r_o \sqrt{\frac{q_s \phi_o}{2\, T_{\|}^{(s)}}} \,. \tag{73}$$

Averaging these rates over the ion orbit, we obtain expressions for the rates of change in the longitudinal and transverse beam temperatures valid for longitudinal beam temperatures in the range

$$\frac{1}{2}\frac{r_o^2}{a^2} \le \frac{T_{\|}^{(s)}}{q_s \phi_o} \le \frac{1}{2}\frac{r_o^2}{r_c^2} \approx 5\times 10^{-2},$$

$$\left.\frac{dT_{\|}^{(s)}}{dt}\right|_{\text{co-moving ions}} \approx \frac{1}{\sqrt{\pi}} \left[\frac{\pi}{4}\,\text{Ln}\left(\frac{r_\times}{r_c}\right) + \frac{r_\times}{a}\,\text{Ln}\left(\frac{2e\ a}{r_\times}\right) - \text{Ln}(2e)\right]$$

$$\times \frac{4}{3}\left(\frac{a}{r_o}\right) q_s \phi_o \left\langle \nu_o^{s/s} \right\rangle_{\text{Vol}} \tag{74}$$

and

$$\left.\frac{d\langle L^2\rangle}{dt}\right|_{\text{co-moving ions}} \approx \frac{1}{\sqrt{\pi}}\,\frac{r_\times r_o}{a^2}\left[\text{Ln}\left(\frac{2a}{e\ r_\times}\right) - \frac{r_\times}{a}\,\text{Ln}\left(\frac{2}{e}\right) - \frac{\pi}{8}\,\frac{a}{r_\times}\left(\frac{r_\times^2 - r_c^2}{r_o^2}\right)\right]$$

$$\times\ L_a^2 \left\langle \nu_o^{s/s} \right\rangle_{\text{Vol}} \tag{75}$$

or, equivalently,

$$\left.\frac{d}{dt}\left(\frac{r_o}{a}\right)\right|_{\text{co-moving ions}} \approx \frac{2}{3\sqrt{\pi}}\,\frac{r_\times}{a}\left[\text{Ln}\left(\frac{2a}{e\ r_\times}\right) - \frac{r_\times}{a}\,\text{Ln}\left(\frac{2}{e}\right) - \frac{\pi}{8}\,\frac{a}{r_\times}\left(\frac{r_\times^2 - r_c^2}{r_o^2}\right)\right]$$

$$\times\ \left\langle \nu_o^{s/s} \right\rangle_{\text{Vol}} \tag{76}$$

where $e \approx 2.718\ldots$ is the base of the Naperian logarithms.

C. Strongly Thermalized Ion Distributions, $\frac{T_{\|}^{(s)}}{q_s\phi_o} \geq \frac{1}{2}\frac{r_o^2}{r_c^2}$

Finally, we consider the regime

$$\frac{T_{\|}^{(s)}}{q_s\phi_o} \geq \frac{1}{2}\frac{r_o^2}{r_c^2} \approx 5\times10^{-2}. \tag{77}$$

In this limit the longitudinal beam temperature is greater than the local value of the transverse beam temperature everywhere in the plasma bulk, and the orbit-averaged rates of change in the beam velocity dispersion are given by

$$\left.\frac{dT_{\|}^{(s)}}{dt}\right|_{\text{co-moving ions}} \approx -\frac{1}{\sqrt{\pi}}\left[\frac{r_\times}{r_c}\,\mathrm{Ln}\left(\frac{2e\,r_c}{r_\times}\right) - \frac{r_\times}{a}\,\mathrm{Ln}\left(\frac{2e\,a}{r_\times}\right)\right]$$

$$\times \frac{4}{3}\left(\frac{a}{r_o}\right) q_s\,\phi_o\,\langle \nu_o^{s/s}\rangle_{\text{Vol}} \tag{78}$$

and

$$\left.\frac{d\langle L^2\rangle}{dt}\right|_{\text{co-moving ions}} \approx \frac{1}{\sqrt{\pi}}\,\frac{r_\times r_o}{a^2}\left[\mathrm{Ln}\left(\frac{2a}{e\,r_\times}\right) - \frac{r_c}{a}\,\mathrm{Ln}\left(\frac{2r_c}{e\,r_\times}\right)\right]$$

$$\times L_a^2\,\langle \nu_o^{s/s}\rangle_{\text{Vol}} \tag{79}$$

or, equivalently,

$$\left.\frac{d}{dt}\left(\frac{r_o}{a}\right)\right|_{\text{co-moving ions}} \approx \frac{2}{3}\,\frac{1}{\sqrt{\pi}}\,\frac{r_\times}{a}\left[\mathrm{Ln}\left(\frac{2a}{e\,r_\times}\right) - \frac{r_c}{a}\,\mathrm{Ln}\left(\frac{2r_c}{e\,r_\times}\right)\right]$$

$$\times \langle \nu_o^{s/s}\rangle_{\text{Vol}} \tag{80}$$

D. Time Evolution of $T_{\|}^{(s)}$ and $\langle L^2 \rangle$

We are now ready to examine the time evolution of $T_{\|}^{(s)}/q_s\phi_o$ and r_o/a. Summing the term describing the rate of increase in $T_{\|}^{(s)}$ due to core collisions [as given by Eq. (59)] with the appropriate term describing the rate of change in $T_{\|}^{(s)}$ due to both collisions between co-moving ions [from Eq. (66), (74), or (78) as appropriate] we obtain an expression for the total rate of change in the longitudinal beam temperature,

$$\left.\frac{dT_{\|}^{(s)}}{dt}\right|_{\text{total}} = \frac{4}{3} G_s\left(T_{\|}^{(s)}/q_s\phi_o, r_o/a\right) \left(\frac{a}{r_o}\right) q_s \phi_o \langle \nu_o^{s/s} \rangle_{\text{vol}} . \qquad (81)$$

The function $G_s\left(T_{\|}^{(s)}/q_s\phi_o, r_o/a\right)$ is displayed in Fig. 11 for deuterium ions in a DT plasma. We see that G_s is weakly varying with both $T_{\|}^{(s)}/q_s\phi_o$ and r_o/a. A further decrease in r_o/a beyond 10^{-4} results in only a very small downward shift relative to the $r_o/a = 10^{-4}$ curve of Fig. 11; while at smaller values of $T_{\|}^{(s)}/q_s\phi_o$ the function G_s goes to

$$G_s \approx d_s + \frac{\sqrt{\pi}}{4} \text{Ln}\left(\frac{a}{r_o}\frac{r_o}{r_c}\right) \qquad \left(T_{\|}^{(s)}/q_s\phi_o < \frac{1}{2}\frac{r_o^2}{a^2}\right) \qquad (82)$$

for any r_o/a. We find that $dT_{\|}^{(s)}/dt$ is positive for all interesting values of $T_{\|}^{(s)}/q_s\phi_o$ and r_o/a. Hence, collisions will result in a monotonic increase of $T_{\|}^{(s)}$ in time.

$$G_d\left(\frac{T_{\|}^{(d)}}{q_d\phi_o}, \frac{r_o}{a}\right) \equiv \frac{\left.\frac{dT_{\|}^{(d)}}{dt}\right|_{total}}{\frac{4}{3}\left(\frac{a}{r_o}\right) q_d\phi_o \langle \nu_o^{d/d} \rangle_{Vol}}$$

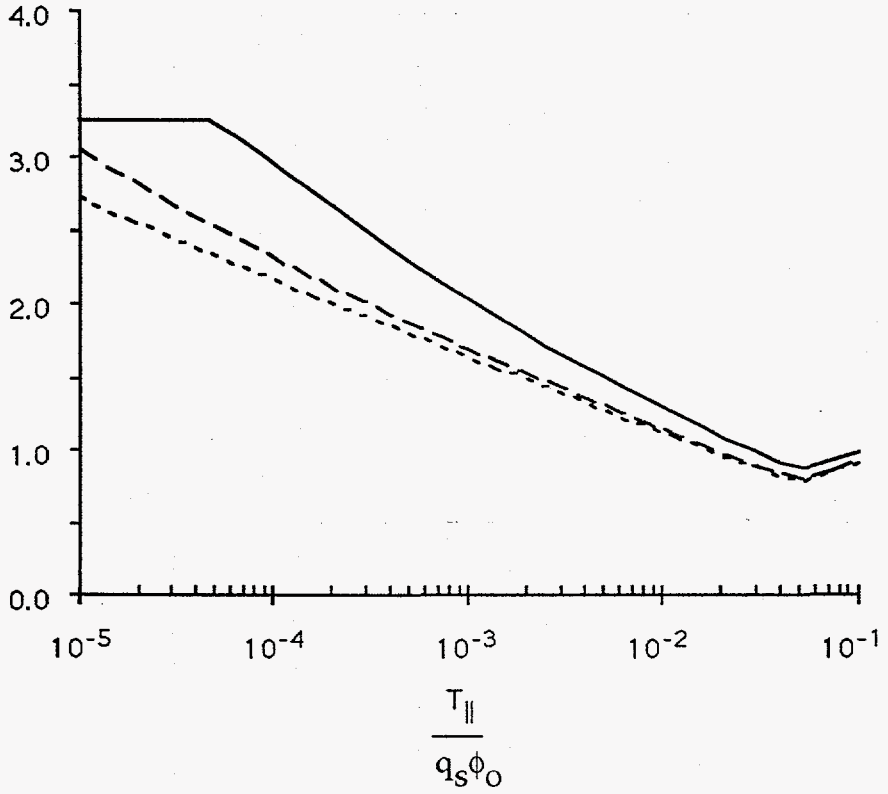

Figure 11. The variation of the longitudinal beam heating rate, including both core collisions and collisions with co-moving ions for deuterons in a DT plasma is displayed for $r_o/a = 10^{-2}$ (solid line), $r_o/a = 10^{-3}$ (long dashes), and $r_o/a = 10^{-4}$ (short dashes).

The behavior of the transverse velocity dispersion as measured by $\langle L^2 \rangle$ is more interesting. Summing the term describing the rate of increase in $\langle L^2 \rangle$ due to core collisions [as given by Eq. (60)] with the appropriate term describing the rate of change in $\langle L^2 \rangle$ due to both collisions between co-moving ions [from Eq. (67), (75), or (79) as appropriate] we obtain an expression for the total rate of change in the $\langle L^2 \rangle$,

$$\left.\frac{d\langle L^2 \rangle}{dt}\right|_{total} = H_s\left(T_{\|}^{(s)}/q_s\phi_o, r_o/a\right) L_a^2 \langle \nu_o^{s/s} \rangle_{Vol} . \qquad (83)$$

The function $H_s(T_{\|}^{(s)}/q_s\phi_o, r_o/a)$ is displayed in Figure 12.

$$H_d(T_{\|}^{(d)}/q_d\phi_o, r_o/a) = \frac{\left.\frac{d\langle L^2\rangle}{dt}\right|_{total}}{L_a^2 \langle \nu_o^{d/d} \rangle_{Vol}}$$

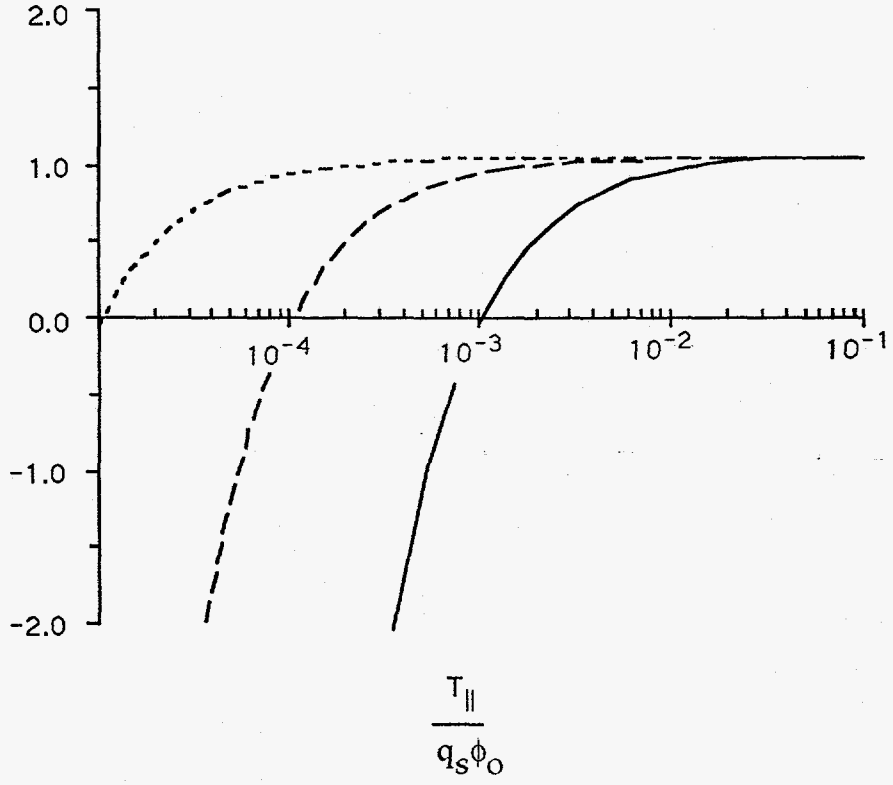

Figure 12. The variation in the total transverse beam heating rate as measured by the rate of increase in $\langle L^2 \rangle$, including both bulk collisions and collisions between co-moving ions, is displayed for deuterium ions in a DT plasma for $r_o/a = 10^{-2}$ (solid line), $r_o/a = 10^{-3}$ (long dashes) and $r_o/a = 10^{-4}$ (short dashes) as a function of $T_{\|}/q_s\phi_o$.

When $T_{\|}^{(s)}/q_s\phi_o$ is small (less than about $0.1\ r_o/a$) collisions between co-moving ions dominate the bulk plasma collisions so that the net effect is rapid decrease in $\langle L^2 \rangle$ (i.e., a rapid decrease in the size of the ion focus, r_o). However, for larger values of $T_{\|}^{(s)}/q_s\phi_o$ the orbit-averaged effect of collisions between co-moving ions weakens, so that both $\langle L^2 \rangle$ and $T_{\|}^{(s)}$ increase monotonically for $T_{\|}^{(s)}/q_s\phi_o > 0.1\ r_o/a$.

The transition from collisional focusing to collisional defocusing can be understood by examining the leading terms in the expression for $d\langle L^2\rangle/dt$ in the moderately thermalized regime, $1/2\, r_o^2/a^2 \le T_\parallel^{(s)}/q_s\phi \le 1/2\, r_o^2/r_c^2$,

$$\left.\frac{d\langle L^2\rangle}{dt}\right|_{total} \approx \left[c_s - \frac{\sqrt{\pi}}{16}\,\frac{q_s\phi_o}{T_\parallel^{(s)}}\left(\frac{r_o}{a}\right)\right] L_a^2 \langle \nu_o^{s/s}\rangle_{Vol}, \qquad (84)$$

where we have used Eq. (73) to express $(r_x/r_o)^2$ as $1/2\, T_\parallel^{(s)}/q_s\phi_o$. It follows that the transition from focusing to defocusing occurs when

$$\frac{T_\parallel^{(s)}}{q_s\phi_o} \approx \frac{\sqrt{\pi}}{16\, c_s}\,\frac{r_o}{a} \approx 0.1\,\frac{r_o}{a}\,. \qquad (85)$$

After initial transients, in which the ion focal radius may decrease in size while $T_\parallel^{(s)}/q_s\phi_o$ increases, the system will reach a state in which $T_\parallel^{(s)}/q_s\phi_o \gtrsim r_o/a$. The longitudinal temperature and ion convergence then satisfy the equations

$$\frac{d}{dt}\left(\frac{T_\parallel^{(s)}}{q_s\phi_o}\right) \approx \frac{4}{3}\left(\frac{r_o}{a}\right)^{-1} \langle \nu_o^{s/s}\rangle_{Vol}\,, \qquad (86)$$

where we have taken $G_d \approx 1$ (valid for and $T_\parallel^{(s)}/q_s\phi_o \sim r_o/a \gtrsim 10^{-2}$, see Fig. 11); and

$$\frac{d}{dt}\left(\frac{r_o}{a}\right) \approx \frac{2}{3}\left(\frac{r_o}{a}\right)^{-1} \langle \nu_o^{s/s}\rangle_{Vol}\,, \qquad (87)$$

where we have taken $H_d \approx 1$ (valid for $T_\parallel^{(s)}/q_s\phi_o \gtrsim r_o/a$, see Fig. 12).

These Equations have the solution

$$\frac{r_o}{a} \approx 2\sqrt{\frac{1}{3}\langle \nu_o^{s/s}\rangle_{Vol}\, t}\,, \qquad (89)$$

and

$$\frac{T_{\|}^{(s)}}{q_s\phi_o} \approx 4\sqrt{\frac{1}{3}<\nu_o^{s/s}>_{Vol} t} + \frac{T_{\|o}^{(s)}}{q_s\phi_o} . \qquad (90)$$

We conclude that collisions between counter-streaming ions will initially lead to rapid thermalization of the distribution of the ion radial velocities (at a rate of order $(a/r_o)<\nu_o^{s/s}>_{Vol}$). Once $T_{\|}^{(s)}$ has increased to the extent that $T_{\|}^{(s)}/q_s\phi_o \gtrsim 0.1\, r_o/a$ this process will be accompanied by the spreading of the ion focus. Finally, when $T_{\|}^{(s)}/q_s\phi_o \gtrsim r_o/a$, the increase in $T_{\|}^{(s)}/q_s\phi_o$ and r_o/a will proceed in concert at a rate of order $(a/r_o)<\nu_o^{s/s}>_{Vol}$. As the ion focus spreads the rate of increase in the focal radius decreases so that it takes a time of order

$$\tau_L^s \sim <\nu_o^{s/s}>_{Vol}^{-1}$$

for the ion distribution function to relax to isotropy and the IEC configuration to be destroyed.

Our conclusions regarding the time evolution of the IEC distribution function is very different from that reached in Ref. 12, where steady-state, beam-like solutions to the kinetic equation were found. Two key reasons for our completely different results are

1) The artificial constraint imposed in Eq. (11) of Ref. 12, which prevents collisions between counter-streaming ion beams from producing any net increase in the velocity dispersion (i.e., heating) of the ion beams;

and

2) The neglect of the dominant term in the evolution of the beam temperature—the increase in the longitudinal velocity dispersion of the beam due to collisions in the plasma core.

When this problem is treated correctly we see that there are no beam-like steady-state solutions to the kinetic equation.

6. Schemes for Maintaining a Strongly Focused Ion Distribution that Don't Work

We have shown that ion-ion collisions will cause the IEC distribution to relax towards an isotropic Maxwellian, and that this process occurs on two time scales. On the fast time scale, $\tau_\varepsilon^s \sim (a/r_0) \langle \nu_0^{s/s} \rangle_{Vol}^{-1}$, the energy distribution relaxes toward a Maxwellian, while on a the somewhat slower time scale, of order $\tau_L^s \sim \langle \nu_0^{s/s} \rangle_{Vol}^{-1}$, the angular distribution relaxes toward isotropy and the ion focus is lost. At the high energies and relatively low volume-averaged densities proposed for IEC devices the ion collisional time scale is rather long— $\langle \nu_0^{d/d} \rangle_{Vol}$ is about 2.2 Hz (as compared to an ion bounce frequency of 1.1 MHz) for the IEC reactor parameters of Table I. Hence, it may be possible to prevent this collisional relaxation through some process that acts only weakly on the ion distribution function. We consider two such schemes which have been proposed by proponents of IEC fusion reactors in this section.

A. Fusion Reaction Rates.

Bussard[10] makes the rather surprising claim that the fusion reactions in an IEC device will remove fuel ions at a rate sufficient to maintain a nearly mono-energetic ion distribution function. In making this claim Bussard recognizes that the fusion reaction rate must be greater than the collisional energy-scattering rate if the loss of fuel ions by fusion reactions is to substantially alter the ion distribution function. In section 5 we showed that the orbit-averaged collisional rate of increase in the beam velocity dispersion is

$$\langle \nu_\varepsilon^d \rangle_{orbit} = \frac{1}{2}\frac{d}{dt}\left(\left.\frac{T_\parallel^{(s)}}{q_s \phi_0}\right|_{total}\right) \approx \frac{2}{3} d_d \left(\frac{a}{r_0}\right) \langle \nu_0^{d/d} \rangle_{Vol}, \qquad (91)$$

while the orbit-averaged fusion rate for the deuterons is given by

$$\langle n_t \langle \sigma v \rangle_{DT} \rangle_{orbit} \approx \frac{v_0}{a} \int_0^a \frac{dr}{v_0} n_t(r) \langle \sigma v \rangle_{D\text{-}T} . \qquad (92)$$

Note that the orbit-averaged fusion rate scales with the core convergence ratio and ion density as $(a/r_0) \langle n_i \rangle_{vol}$ — that is, in exactly the same manner as the rate of increase in the longitudinal velocity dispersion. We computed the orbit-averaged fusion rate following the methods described in section 3. This rate is

plotted together with the orbit-averaged energy diffusion rate versus the potential well depth in Fig. 13. We see that the orbit-averaged energy diffusion rate substantially exceeds the orbit-averaged fusion rate at all potential well depths considered (5 kV $\leq \phi_0 \leq$ 275 kV). We conclude that fusion reactions rates are not sufficient to materially effect the form of the ion energy distribution function.

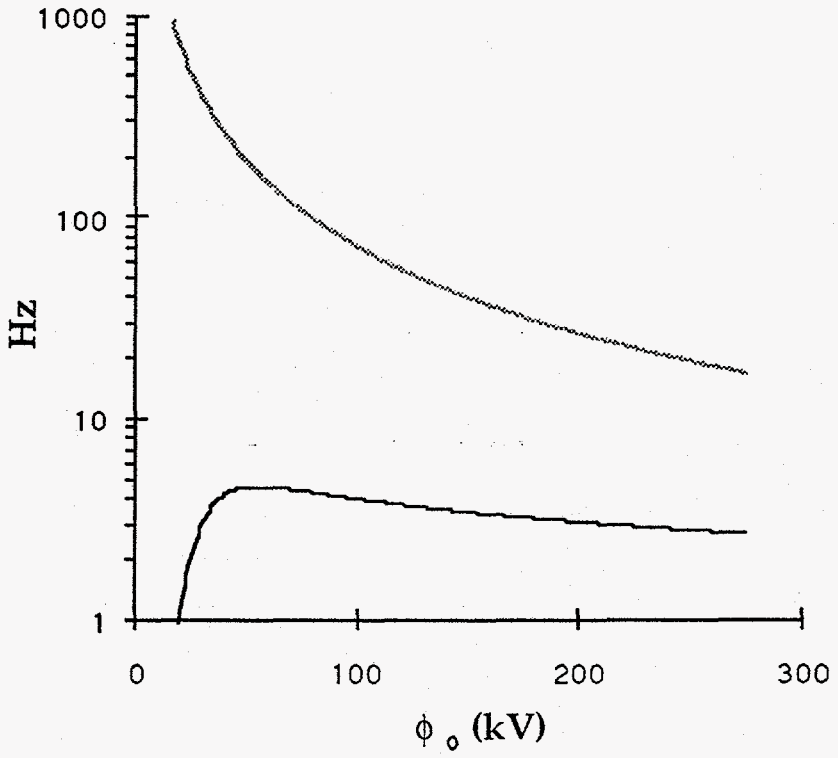

Figure 13. Orbit-averaged fusion rate coefficient (black curve) and orbit-averaged energy diffusion rate (grey curve) vs. potential well depth, ϕ_o, for deuterons in a DT plasma. The ion density, convergence ratio, etc. are taken from Table I. The relative magnitude of fusion and collisional rates are insensitive to the choice of n_i and r_o/a.

The rate of decay of the ion anisotropy is slower than the rate at which the ion energy distribution relaxes to a Maxwellian. Hence, one might hope that the loss of fuel ions through fusion reactions could maintain the ion anisotropy. We may estimate the resulting ion core radius by replacing "t" in Eq. (89) with the inverse of the orbit-averaged fusion reaction rate. After a bit of manipulation, we can put this estimate in the form

$$\frac{r_o}{a} \approx \frac{1}{d_d} \frac{\langle v_{\parallel}^d \rangle_{orbit}}{\langle n_t \langle \sigma v \rangle_{DT} \rangle_{orbit}} >> 1. \qquad (93)$$

We conclude that the removal of fuel ions by fusion reactions occurs at a rate that is insufficient to maintain an ion focus. The situation regarding maintenance of the ion anisotropy is essentially the same as that regarding maintenance of a non-Maxwellian ion energy distribution because the orbit-averaged fusion rate decreases as the ion focus spreads, thereby making fusion reactions less effective as a mechanism for removing fuel ions before they are scattered further in angle.

B. Maintenance of Ion Anisotropy with a "Cold" Plasma Mantle

The basic idea inspiring the work of Rosenberg and Krall was that it might be possible to control the ion distribution function in an IEC device by manipulating the ion distribution function in the neighborhood of the ion injection point. In section 5 we demonstrated that the calculation performed in Ref. 12 is in error, and that collisions between ions with low relative velocities cannot prevent thermalization of the ion distribution function. However, perhaps this only demonstrates that the wrong problem was addressed both in section 5 and in Ref. 12. In this subsection we consider the related problem in which the ion distribution function at the injection point is treated as a boundary condition. We are then able to force the transverse temperature to go to zero at the lip of the potential well, which we take at $(\varepsilon - L^2/2m_s a^2) = 0$, rather than at $(\varepsilon - L^2/2m_s a^2) = +q_s\phi_o$, so that this boundary condition will have greater influence on the distribution of trapped ions.

It is convenient to adopt as velocity-space co-ordinates u, the particle speed normalized to the thermal velocity, and μ, the cosine of the angle that the particle makes with the normal when it strikes the surface of spherical square well potential. Note that both of these velocity-space co-ordinates can be expressed as functions of ε and L^2,

$$\mu = \pm \sqrt{1 - \frac{L^2}{2m_s a^2(\varepsilon + q_s\phi_o)}} \qquad (94)$$

$$u = \sqrt{\frac{2(\varepsilon + q_s\phi_o)}{T_s}} \qquad (95)$$

so that u and μ are themselves constants of the single particle motion. We assume that the steady-state ion distribution function is nearly an isotropic Maxwellian (and verify this assumption *a posteriori*) so that we may use the usual

test-particle collision operator. In the high-velocity limit ($u \gtrsim 2$) the steady-state kinetic equation may then be written as

$$\frac{\partial^2 f}{\partial u^2} + \left(u - \frac{1}{u}\right)\frac{\partial f}{\partial u} + \frac{\partial}{\partial \mu}\left(1 - \mu^2\right)\frac{\partial f}{\partial \mu} = 0 . \tag{96}$$

We look for solutions in the form

$$f(u, \mu) = \sum_L f_L(u)\, P_L(\mu) \tag{97}$$

where the $P_L(\mu)$ are Legendre Polynomials of index L, and the $f_L(u)$ satisfy

$$\frac{d^2 f_L}{du^2} + \left(u - \frac{1}{u}\right)\frac{df_L}{du} + L(L+1)\, f_L = 0 . \tag{98}$$

We solve this equation on the domain $0 \le u \le u_{max} = \sqrt{2q_s\phi_o/T_s}$, taking as our boundary condition a plasma with finite phase-space density and zero velocity spread at the ion injection point,

$$f(u_{max}, \mu) = \frac{f_o}{2}\left[\, \delta(\mu - 1) + \delta(\mu + 1)\,\right] . \tag{99}$$

Expanding this boundary condition in a Legendre series we obtain

$$f_L(u_{max}) = \frac{f_o}{2}(2L + 1) \qquad \text{for L even,} \tag{100}$$

and

$$f_L(u) = 0 \qquad \text{for L odd.} \tag{101}$$

The solutions of the kinetic equation with this boundary condition are shown in Fig. 14 for the first four even Legendre harmonics. We see that our highly anisotropic boundary condition has an appreciable effect on the distribution function only at the highest speeds, $u \gtrsim 2$. The bulk of the phase-space density is contained in $f_0(u)$, an isotropic Maxwellian, providing the *a posteriori* justification for the use of the test particle collision operator.

The L=0 Legendre harmonic is the sum of a Maxwellian plus a small constant term required to match the boundary condition at $u=u_{max}$. The density and temperature of this Maxwellian must be determined from consideration of

energy and particle balance in analogy to the Pastukhov solution of the problem of electron confinement in magnetic mirrors.[22, 23]

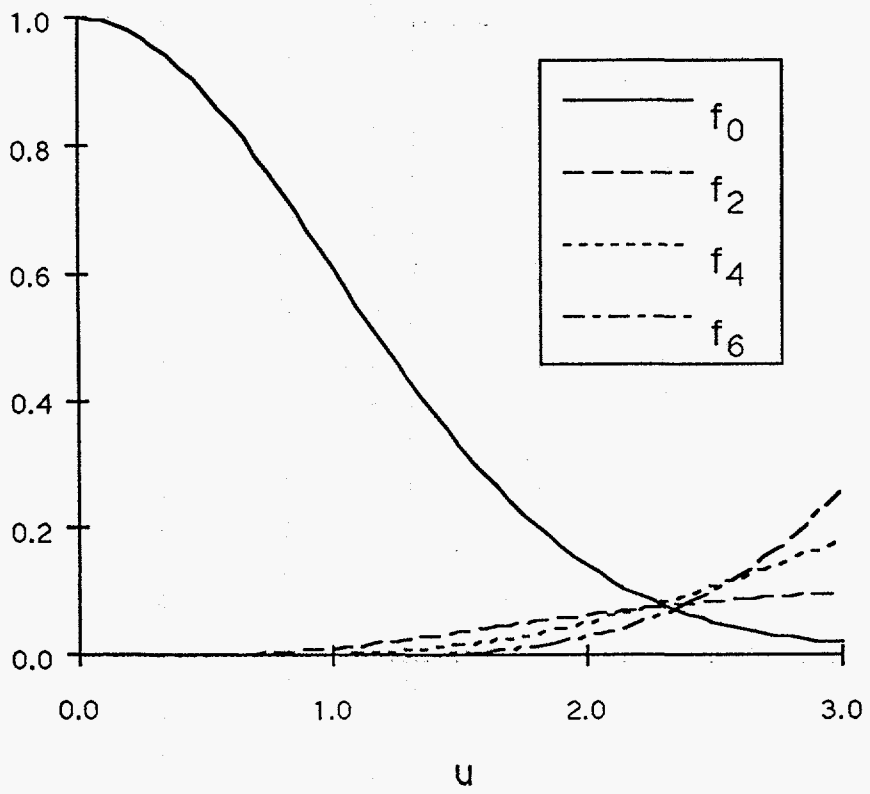

Figure 14. The first four even Legendre harmonics of the steady-state ion distribution function when a zero transverse temperature boundary condition is applied at $u=u_{max}$.

Another way of displaying this information is to compute the effective radius of the ion focus from the root-mean-square value of the distance of closest approach at each ion speed,

$$r_{eff}(u) \equiv a\sqrt{\frac{3}{2}<1-\mu^2>(u)} = a\sqrt{\frac{f_0(u)-1/5\,f_2(u)}{f_0(u)}}\,. \qquad (102)$$

This effective ion focal radius is displayed as a function of ion speed in Fig. 15. We see that there is essentially no ion focusing at speeds less than twice the ion thermal velocity. We conclude that it is not possible to maintain a strongly anisotropic ion distribution function in an IEC device solely by controlling the form of the ion distribution function at the ion injection point.

---

[22]V. P. Pastukhov, Nucl. Fusion **14**, 3 (1974).

[23]R.H. Cohen M.E. Rensink, A.A. Mirin and T.A. Cutler, Nucl. Fusion **18**, 1229, (1978).

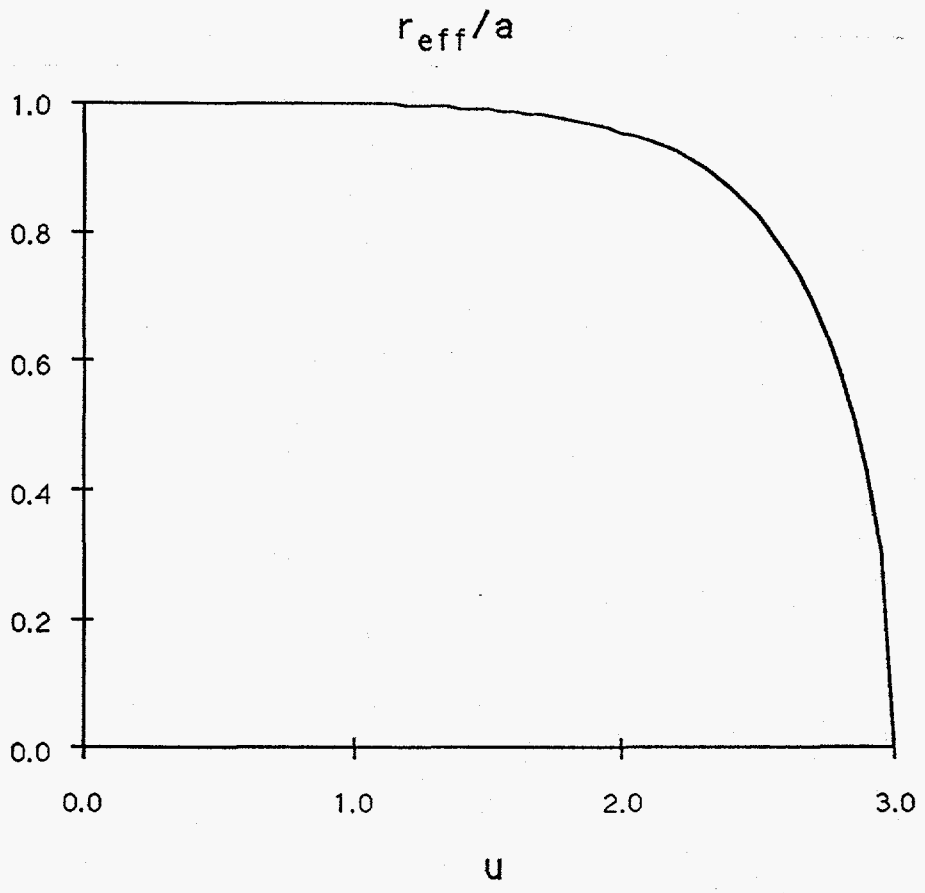

Figure 15. The effective radius of the ion focus is displayed as a function of the ion speed for the steady-state ion distribution function of Fig. 14 with a zero transverse velocity boundary condition applied at $u_{max} = 3$.

7. Schemes for Maintaining a Strongly Focused Ion Distribution That Work, but Require too Much Power

We have shown that two mechanisms proposed by proponents of IEC systems to maintain a strongly non-thermal ion distribution function will not be effective. In the absence of intervention the ion distribution function will thermalize in an ion-ion collision time. In this section we propose two approaches for maintaining a strong ion focus in an IEC system. These approaches are based on the assumption that some means can be found to control the ion confinement time such that ions will be lost before they have time to fully thermalize. The ion lifetime is in fact limited in electrostatic traps that use grids (due to the finite grid transparency), and in Penning traps (due the leakage of ions through the poles of the trap).

A. Power Cost of Maintaining a Nearly Mono-Energetic Ion Distribution

We first consider IEC systems in which ions are removed at a rate sufficient to maintain a nearly mono-energetic ion distribution function. A potential benefit of such an approach is that the collisions between co-moving ions can be used to control the quality of the ion focus if we choose to maintain the parallel velocity dispersion (as measured by $T_{\|}^{(d)}/q_d\phi_o$) such that $d\langle L^2\rangle/dt \approx 0$ (see Fig. 12). This requires $T_{\|}^{(d)}/q_d\phi_o \approx 0.1\, r_o/a$. The ion lifetime required too achieve this velocity dispersion is

$$\tau_{pump} = \frac{T_{\|}^{(s)}}{\left.\frac{dT_{\|}^{(s)}}{dt}\right|_{collisions}} \approx 0.062 \left(\frac{r_o}{a}\right)^2 \frac{1}{\langle \nu_o^{s/s} \rangle_{Vol}} , \qquad (103)$$

where we have taken $H_d(T_{\|}^{(d)}/q_d\phi_o, r_o/a) \approx 1.21$ consistent with $T_{\|}^{(d)}/q_d\phi_o = 1\times10^{-3}$ and $r_o/a = 1\times10^{-2}$. For the IEC reactor parameters of Table I we obtain $\tau_{pump} \approx 3.9\ \mu s$ (or about four ion transit times).

The energy required to remove an ion is at least equal to the energy spread in the ion distribution,

$$\varepsilon_{pump} \gtrsim m_s v_s \langle \Delta v_{\|}^2 \rangle^{1/2} = \sqrt{2\, q_s\phi_o\, T_{\|}^{(s)}} \approx 0.45\, q_s\phi_o \sqrt{\frac{r_o}{a}} . \qquad (104)$$

Assuming $\phi_o \approx 50.66$ keV to maximize the DT fusion rate coefficient and $r_o/a \approx 1\times10^{-2}$, this comes to 2.3 keV to remove each ion. The total power required to maintain the ion distribution function is then

$$P_{pump} \gtrsim \frac{N_i\,\varepsilon_{pump}}{\tau_{pump}} \approx 7.2\,q\phi_o\,N_i\,\left(\frac{r_o}{a}\right)^{3/2} \langle \nu_o^{s/s} \rangle_{Vol}\,, \qquad (105)$$

which comes to about 20 GW for the IEC reactor of Table I (which produces 590 MW of fusion power). The power balance in this operating mode can be characterized by

$$Q \le \frac{P_{fusion}}{P_{pump}} \approx 6.2\times10^{-2}\,\frac{Y_{DT}}{q_d\phi_o}\,\sqrt{\frac{r_o}{a}}\,\frac{\langle n_d \rangle_{Vol}\,\langle \sigma v \rangle_{DT}^{eff}}{\langle \nu_o^{d/d} \rangle_{Vol}}\,. \qquad (106)$$

For the Reference IEC reactor of Table I this upper limit on Q is $Q \lesssim 0.028$. In fact, Q will certainly be well below this limit as this estimate does not take account of the power required to maintain the potential well and support energy losses in the electron channel.

Apart from weak dependencies through $G_s(T_{\|}^{(s)}/q_s\phi_o, r_o/a)$, this estimate of the upper limit on the fusion gain, Q, depends only on the potential well depth, ϕ_o, and the ion convergence ratio, a/r_o. For DT plasmas,

$$Q \sim \frac{\langle \sigma v \rangle_{DT}^{eff}}{q_d\phi_o \langle \nu_o^{d/d} \rangle_{Vol}}$$

is a very slowly increasing function of ϕ_o for $\phi_o \ge 50$ kV, whose value has increased by 10% as ϕ_o is increased from 50 kV to 75 kV; and by an additional 10% as ϕ_o is increased to 300 kV. Assuming that there must be some penalty to increasing ϕ_o, we take $\phi_o \approx 75$ kV, yielding a 10% improvement in Q (to $Q \lesssim 0.031$). Surprisingly, we see that fusion gain increases with **decreasing** ion convergence ratio. Decreasing the convergence ratio to $a/r_o \approx 10$ (which we take to be the lower limit for an IEC system) produces a further increase in this upper-limit on the fusion gain to $Q \lesssim 0.097$.

These very disappointing limits on the fusion gain follow from the fact that the averaged fusion rate is small compared to the averaged collisional rate [see Eq. (106) and Fig. 13], so that the power required to maintain the non-thermal, mono-energetic IEC ion distribution is too high. This suggests that we

relax our requirements on the ion distribution function, and examine the limit in which the ion energy distribution is allowed to thermalize in energy, while maintaining strong ion convergence.

B. Power Cost of Maintaining a Strongly Anisotropic Ion Distribution

It was shown in section 3 that the fusion rate coefficient for a nearly mono-energetic ion distribution function peaks at a value that is not substantially greater than the peak in the fusion rate coefficient for Maxwellian plasmas. Given the relatively small penalty in fusion power from allowing the ion energy distribution to thermalize, one is led to consider an operating mode in which the ion speed distribution is allowed to relax to a Maxwellian, while ions are removed at a rate sufficient to maintain the ion anisotropy and a strong ion convergence ratio. The ion lifetime required to maintain a given convergence ratio is

$$\tau_{pump} \approx \frac{3}{4}\left(\frac{r_o}{a}\right)^2 \frac{1}{\langle \nu_o^{s/s} \rangle_{Vol}} \quad . \tag{107}$$

If we assume a temperature of 70 keV to maximize the Maxwellian-averaged fusion rate coefficient, while maintaining the same average density as the reactor in Table I, this calculation yields a required ion lifetime of 75 μs.

A potential well depth $q_s\phi_o \gtrsim 3/2\ T_s$ will be required to confine the ions, which have a mean longitudinal energy of $1/2\ T_s$. We can imagine pumping these ions using charge-exchange on a neutral beam with an energy $1/2\ T_s$ at an energy cost of

$$\varepsilon_{pump} \approx \frac{1}{2}\ T_s \approx 35\ keV \tag{108}$$

for $T_s \approx 70$ keV. Hence, the required pumping power is

$$P_{pump} \geq \frac{2}{3}\ N_i\ T_i \left(\frac{a}{r_o}\right)^2 \langle \nu_o^{s/s} \rangle_{Vol} \tag{109}$$

which comes to 15 GW for the IEC reactor of Table I.

Assuming a Maxwellian distribution in ion energy together with the same strongly peaked distribution in angular momentum, the ion number density is less peaked radially than it is for the IEC distribution of section 2. Hence, the fusion power is somewhat smaller,

$$P_{fusion} \approx \frac{\sqrt{\pi}}{9} \langle n_i \rangle^2 \, V \, Y_{DT} \left(\frac{a}{r_o} \right) \langle \sigma v \rangle_{DT}^{Max} , \qquad (110)$$

or about 125 MW for the reactor parameters of Table I at an ion temperature $T_i \approx 70$ keV. The fusion power balance is now characterized by

$$Q \leq \frac{P_{fusion}}{P_{pump}} \approx 0.30 \, \frac{Y_{DT}}{T_i} \left(\frac{r_o}{a} \right) \frac{\langle n_d \rangle_{Vol} \langle \sigma v \rangle_{DT}^{max}}{\langle \nu_o^{d/d} \rangle_{Vol}} . \qquad (111)$$

For the IEC reactor parameters of Table I this yields $Q \lesssim 8.1 \times 10^{-3}$. However, can we obtain a factor of 1.2 improvement in Q by reducing T_t to ~40 keV, increasing our limit on Q to $Q \lesssim 9.5 \times 10^{-3}$. Further improvements in Q require a reduction in the ion convergence ratio, a/r_o. The scaling is now more favorable [being linear in (r_o/a)]. At the minimum convergence ratio consistent with an IEC configuration, $a/r_o \approx 10$, we find the optimal fusion power balance, $Q \lesssim 0.095$. This is a particularly disappointing result in light of the fact that the upper limit on Q due to ion pumping goes to $Q \lesssim \infty$ if we continue to assume that a potential well can be formed at little cost in power while abandoning the IEC concept and letting $a/r_o \rightarrow 1$.

We conclude that at high convergence ratio there is an advantage to operation with nearly mono-energetic distributions, while at low convergence ratio there is an advantage in allowing the ion energy distribution to thermalize. However, we always find that the optimal IEC reactor power balance occurs at the lowest allowed ion convergence ratio, a/r_o, and that the power required to maintain the ion distribution function is that retains the defining characteristic of an IEC system ($a/r_o \gtrsim 10$) is at least an order of magnitude greater than the fusion power that this system might produced. Reactor studies indicate that an economic DT fusion power reactor requires much more favorable energy balance, $Q \geq 10$. Hence, there appears to be no prospect that an economic electrical power generating reactor can be developed based on an inertial electrostatic confinement scheme.

8. Conclusions

We have presented a model for the ion distribution function in an inertial electrostatic confinement system. This model is shown to reproduce the essential features of IEC systems—electrostatic confinement, strong central peaking of the ions, and a mono-energetic energy distribution. Using this model distribution function we are able to test key claims made by proponents of IEC systems. We find:

1) After averaging over collision angle and volume, the peak in the effective fusion rate coefficient for DT ($\langle\sigma v\rangle^{eff}_{D\text{-}T} \approx 9.0\times10^{-22}m^3/s$ at $\phi_o \approx 50$ keV for the IEC distribution vs. $8.9\times10^{-22}m^3/s$ at T = 75 keV for a thermal distribution) or D^3He ($\langle\sigma v\rangle^{eff}_{D^3He} \approx 2.8\times10^{-22}m^3/s$ at $\phi_o \approx 140$ keV vs. $2.5\times10^{-22}m^3/s$ at T = 250 keV[16]) reactions are not significantly higher than the peak in the corresponding thermal rate coefficient.

2) Ion/ion collisions will cause the ion distribution function to relax to a Maxwellian in energy at a rate that is enhanced relative to the ion-ion collision frequency (evaluated at the volume-averaged density) by one power of the convergence ratio, a/r_o.

3) Ion/ion collisions will cause a further relaxation to an isotropic ion distribution on the ion-ion collisional time-scale (evaluated at the volume-averaged density).

4) The means of preventing this relaxation of the ion distribution function so far proposed by proponents of IEC schemes are not effective.

5) The energy cost of maintaining an anisotropic ion distribution function through control of the ion lifetime is at least an order of magnitude greater than the fusion power that would be produced by the IEC device.

This analysis is based on a particular model ion distribution function, while the reactor operating point has been optimized over the parameters of this model. It is possible that a more attractive power balance could be obtained by further optimization of the form of the ion distribution function. A serious effort to perform such an optimization would require the development of a bounce-averaged Fokker Planck code in (ε, L^2)-space. However, it seems most unlikely that such optimization will increase Q by the factor of 100 required to achieve an acceptable recirculating power fraction for an economic power plant. Hence, we conclude that inertial electrostatic confinement shows little promise as a basis for the development of commercial electrical power plants.

The analysis does not place a lower-limit on the unit size of an IEC reactor. Such a lower limit on the unit size will (persumably) follow from an analysis of electron energy confinement and the energy cost of maintaining the spherical potential well. This leaves open the possibility that IEC based reactors may prove useful as means of generating a modest flux of 14 MeV neutrons for applications other than power generation, such as such as assaying, neutron imaging, materials studies, and isotope production. In such applications a small unit size ($P_{fusion} \lesssim 1$ kW) and, hence, smaller unit cost might compensate for modest values of Q ($Q \gtrsim 10^{-3}$).

Acknowledgments

This work was motivated by presentations of R.W. Bussard and N.A. Krall on the promise of IEC-based fusion reactors. It has benefited from stimulating discussions with B. Afeyan, D.C. Barnes, R.H. Cohen, T.J. Dolan, R. Fonck, T.K. Fowler, L.L. Lodestro, G.H. Miley, J. Perkins and D. Ryutov. Particular thanks are due to S.W. Haney for providing the numerical solution to the ion kinetic equation described in Sec. 6. This work was performed under the auspices of the U.S. Department of Energy by the Lawrence Livermore National Laboratory under contract number W–7405–ENG–48.

Appendix A. Collisional Rate Coefficients for a Mono-Energetic IEC Distribution Function.

In this appendix we compute the rate of increase in the transverse and longitudinal velocity dispersion, $<\Delta v_\perp{}^2>$ and $<\Delta v_\parallel{}^2>$, for a test particle of species s and velocity $\mathbf{v} = v_r \hat{\mathbf{e}}_r$ colliding with field particles of species s'. The distribution function of the field particles is taken to be the mono-energetic IEC model distribution function defined in section 2. Since the model IEC velocity distribution function varies as a function of radius, we expect these rates of increase in the longitudinal and transverse velocity dispersion to vary with radius.

Rosenbluth, McDonald, and Judd[24] give a compact expression for the rate of increase in the velocity dispersion due to Coulomb collisions. Following these authors we use the symbols $<\Delta v_\perp{}^2>$ and $<\Delta v_\parallel{}^2>$ in this appendix only to denote the rate of increase in the velocity dispersion rather than the velocity dispersion itself. In the main text these symbols are used to denote the velocity dispersion. These rates are given by:

$$<\Delta v \Delta v>_s = \sum_{s'} <\Delta v \Delta v>_{ss'}$$

where $<\Delta v \Delta v>_{ss'}$, the rate of increase in the velocity dispersion in species s due to collisions with particles of species s', is given by

$$<\Delta v \Delta v>_{ss'} = \frac{4\pi q_s{}^2 q_{s'}{}^2 \, \mathrm{Ln}\, \Lambda_{ss'}}{m_s{}^2} \frac{\partial^2}{\partial v v} \int d^3v' \, f_{s'}(v') \, |v - v'| \,).$$

Defining a characteristic speeds v_s for species s, and using the vector identity

$$\frac{\partial^2}{\partial v v} \, | \, v - v' \, | \, = \frac{\overleftrightarrow{I} - \hat{w}\,\hat{w}}{|w|},$$

we can write the rate of increase in the velocity dispersion as

$$<\Delta v \Delta v>_{ss'} = \nu_o^{s/s'} v_s{}^2 \frac{v_s}{n_{s'}} \int d^3v' \, f_{s'}(v') \, \frac{\overleftrightarrow{I} - \hat{w}\,\hat{w}}{|w|},$$

---

[24] M.N. Rosenbluth, W.M. MacDonald, and D.L. Judd, Phys. Rev. 107, 1 (1957). See especially Eqs. (18) and (19).

where $\mathbf{w} \equiv (\mathbf{v} - \mathbf{v}')$, $\hat{\mathbf{w}} \equiv \mathbf{w}/|\mathbf{w}|$, $\overleftrightarrow{I}$ is the identity tensor and, following Book,[16] we define

$$\nu_o^{s/s'} \equiv \frac{4\pi q_s^2 q_{s'}^2 n_{s'} \, \mathrm{Ln}\, \Lambda_{ss'}}{m_s^2 v_s^3} \, .$$

The mono-energetic IEC distribution evaluated at radius r may be written in spherical co-ordinates as

$$f_{s'}(\mathbf{v}') = \frac{n_{s'}(r)}{2\pi v_{s'}^2} \frac{H(|\mu'| - \mu_o)}{2(1 - \mu_o)} \delta(v' - v_{s'}) \, ,$$

where principle axis of the spherical co-ordinates is taken parallel to $\hat{\mathbf{e}}_r$, μ' is the cosine of the angle between $\mathbf{v}'$ and $\hat{\mathbf{e}}_r$, $n_{s'}(r)$ is the local value of the field ion density as given by Eq. (10),

$$v_{s'} \equiv \sqrt{\frac{2q_{s'}\phi_o}{m_{s'}}}$$

and

$$\mu_o = \begin{cases} 0 & r \le r_o \\ \sqrt{1 - r_o^2/r^2} & r > r_o \end{cases}$$

The integral over the field ion speed is easily performed, yielding

$$\langle \Delta v \Delta v \rangle_{ss'} = \nu_o^{s/s'} v_s^2 \frac{v_s}{v_{s'}} \int_{-1}^{1} d\mu' \int_0^{2\pi} \frac{d\phi}{2\pi} \frac{H(|\mu'| - \mu_o)}{2(1 - \mu_o)} \frac{\overleftrightarrow{I} - \hat{\mathbf{w}}\,\hat{\mathbf{w}}}{\sqrt{1 + u^2 - 2\mu' u_{s'}}}$$

where

$$u_{s'} \equiv v_s / v_{s'} \, .$$

The only dependence on the azimuthal angle, ϕ, comes through the unit vector

$$\hat{w} = \frac{(u_{s'} - \mu')\,\hat{e}_r - \sqrt{1-\mu'^2}\,(\hat{e}_1 \cos\phi + \hat{e}_2 \sin\phi)}{\sqrt{1 + u_{s'}^2 - 2\mu' u_{s'}}}.$$

It follows that the integral over azimuthal angle acts only on the diads, yielding

$$\int_0^{2\pi} \frac{d\phi}{2\pi} \left(\overleftrightarrow{I} - \hat{w}\,\hat{w}\right) = \left(1 - \frac{1}{2}\frac{1-\mu'^2}{(u_{s'}^2 + 1 - 2\mu' u_{s'})}\right)\left(\overleftrightarrow{I} - \hat{e}_r\,\hat{e}_r\right)$$

$$+ \left(\frac{1-\mu'^2}{(u_{s'}^2 + 1 - 2\mu' u_{s'})}\right) \hat{e}_r\,\hat{e}_r .$$

Because there is only one preferred direction in velocity space ($\hat{e}_r$) we are able to write $\langle \Delta v \Delta v \rangle_s$ in the form

$$\langle \Delta v \Delta v \rangle_{ss'} = \frac{1}{2} \langle \Delta v_\perp^2 \rangle_{ss'} \left(\overleftrightarrow{I} - \hat{e}_r\,\hat{e}_r\right) + \langle \Delta v_\parallel^2 \rangle_{ss'}\, \hat{e}_r\,\hat{e}_r ,$$

where the rate of increase in the transverse velocity dispersion is given by

$$\langle \Delta v_\perp^2 \rangle_{ss'} = 2\,\nu_o^{s/s'} v_s^2 \frac{v_s}{v_{s'}} \int_{-1}^{1} d\mu' \frac{H(|\mu'| - \mu_o)}{2(1-\mu_o)}$$

$$\times \left[\left(\frac{1}{\sqrt{u_{s'}^2 + 1 - 2\mu' u_{s'}}} - \frac{1}{2}\frac{1-\mu'^2}{(u_{s'}^2 + 1 - 2\mu' u_{s'})^{3/2}}\right)\right],$$

and the rate of increase in the longitudinal velocity dispersion is given by

$$\langle \Delta v_\parallel^2 \rangle_{ss'} = \nu_o^{s/s'} v_s^2 \frac{v_s}{v_{s'}} \int_{-1}^{1} d\mu' \frac{H(|\mu'| - \mu_o)}{2(1-\mu_o)} \left(\frac{1-\mu'^2}{(u_{s'}^2 + 1 - 2\mu' u_{s'})^{3/2}}\right).$$

Two integrals remain to be evaluated,

$$I_1(\mu, u) = \frac{1}{2(1-\mu_o)} \int_{\mu}^{} \frac{1}{\sqrt{1+u^2-2\mu' u}}$$

$$= -\frac{1}{u} \frac{\sqrt{1+u^2-2\mu u}}{2(1-\mu_o)} ,$$

and

$$I_2(\mu, u) = \frac{1}{2(1-\mu_o)} \int_{\mu}^{} \frac{1-\mu'^2}{(1+u^2-2\mu' u)^{3/2}}$$

$$= \frac{1-\mu^2}{u} \frac{(1+u^2-2\mu u)^{-1/2}}{2(1-\mu_o)}$$

$$- \frac{2\mu}{u^2} \frac{(1+u^2-2\mu u)^{1/2}}{2(1-\mu_o)}$$

$$- \frac{2}{3u^3} \frac{(1+u^2-2\mu u)^{3/2}}{2(1-\mu_o)} .$$

Combining these results, we obtain the rate of increase in the transverse velocity dispersion,

$$\langle \Delta v_\perp^2 \rangle_s = 2 \sum_{s'} \nu_o^{s/s'} v_s^2 \frac{v_s}{v_{s'}} I_\perp(\mu_o, u_{s'})$$

and the rate of increase in the longitudinal velocity dispersion ,

$$\langle \Delta v_\parallel^2 \rangle_s = \sum_{s'} \nu_o^{s/s'} v_s^2 \frac{v_s}{v_{s'}} I_\parallel(\mu_o, u_{s'}) ,$$

where

$$I_{\perp}(\mu_o, u) \equiv \left\{ \frac{I_1(1,u) - I_1(\mu_o,u) + I_1(-\mu_o,u) - I_1(-1,u)}{2\,(1-\mu_o)} \right.$$

$$\left. - \frac{I_2(1,u) - I_2(\mu_o,u) + I_2(-\mu_o,u) - I_2(-1,u)}{4\,(1-\mu_o)} \right\}$$

and

$$I_{\parallel}(\mu_o, u) \equiv \frac{I_2(1,u) - I_2(\mu_o,u) + I_2(-\mu_o,u) - I_2(-1,u)}{2\,(1-\mu_o)} .$$

For $\mu_o \approx 1$ (corresponding to radial locations in the bulk plasma, where $r >> r_o$ the IEC distribution function corresponds to two counter-streaming beams. We can remove the contribution of collisions between co-moving particles from the collision integrals, $I_{\perp}$ and $I_{\parallel}$ by replacing the upper limit of 1 in the integrals I_1 and I_2 with $\mu_c < 1$. This results in the modified collision integrals

$$I'_{\perp}(\mu_o, u\,|\mu_c) \equiv \left\{ \frac{I_1(\mu_c,u) - I_1(\mu_o,u) + I_1(-\mu_o,u) - I_1(-1,u)}{2\,(1-\mu_o)} \right.$$

$$\left. - \frac{I_2(\mu_c,u) - I_2(\mu_o,u) + I_2(-\mu_o,u) - I_2(-1,u)}{4\,(1-\mu_o)} \right\}$$

and

$$I'_{\parallel}(\mu_o, u\,|\mu_c) \equiv \frac{I_2(\mu_c,u) - I_2(\mu_o,u) + I_2(-\mu_o,u) - I_2(-1,u)}{2\,(1-\mu_o)} .$$

The angular width of the counter-streaming beams, μ_o, increases towards the plasma core ($r \le r_o$). Hence, the proper choice of μ_c involves a trade-off between eliminating the effects of collisions between co-moving particles over most of the plasma bulk, while minimizing the effect of the cut-off on the collision operator near the plasma core where the ion distribution function becomes isotropic, and the ansatz of counter-streaming beams breaks down. Our experience indicates that $\mu_c \approx 0.95$ provides an adequate compromise.

Finally, we note that

$$\lim_{\mu_o \to 1} \left[I'_{\perp}(\mu_o, u) \right] = \frac{1}{2} \frac{1}{u_{s'} + 1}$$

and

$$\lim_{\mu_o \to 1} \left[I'_{\parallel}(\mu_o, u) \right] \approx \frac{1}{2} \frac{1 - \mu_o}{(u_{s'} + 1)^3} \to 0 .$$